Theoretical modeling of ultrafast relaxation dynamics in conventional metals: A Boltzmann transport equation approach

A thesis

Submitted in partial fulfillment for the Degree of

Master of Science

as a part of Integrated Ph.D. programme in

Materials Science

by

Aashish Kumar

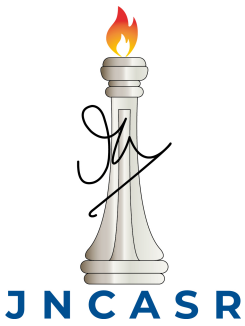

Chemistry and Physics of Materials Unit

Jawaharlal Nehru Centre for Advanced Scientific Research

Bangalore - 560 064

March 2022

To my parents and brother

DECLARATION

I hereby declare that the matter embodied in the thesis entitled "**Theoretical modeling of ultrafast relaxation dynamics in conventional metals: A Boltzmann transport equation approach**" is the result of investigations carried out by me at the Theoretical Sciences Unit, Jawaharlal Nehru Centre for Advanced Scientific Research, Bangalore, India under the supervision of Prof. N.S. Vidhyadhiraja and that it has not been submitted elsewhere for the award of any degree or diploma.

In keeping with the general practice in reporting scientific observations, due acknowledgement has been made whenever the work described is based on the findings of other investigators.

Aashish Kumar

CERTIFICATE

I hereby certify that the matter embodied in this thesis entitled "**Theoretical modeling of ultrafast relaxation dynamics in conventional metals: A Boltzmann transport equation approach**" has been carried out by Mr. Aashish Kumar at the Theoretical Sciences Unit, Jawaharlal Nehru Centre for Advanced Scientific Research, Bangalore, India under my supervision and that it has not been submitted elsewhere for the award of any degree or diploma.

Prof. N.S. Vidhyadhiraja
(Research Supervisor)

Acknowledgements

First of all I would like to convey my wholehearted thanks to my supervisor Prof. N. S. Vidhyadhiraja for all his constant guidance, support, motivation, and valuable suggestions throughout the process. He is great as a teacher and a mentor. It was a great pleasure to work with him. It has been a true privilege to have him as my advisor.

I am also thankful to our collaborator Dr. N Kamaraju from IISER Kolkata for various fruitful and enlightening discussions. I thank him for being the source of many insights. Interacting with him has always helped me gain a better understanding of the problem.

I would like to extend my gratitude to Prof. Shobhana Narasimhan, Prof. U. V. Waghmare, Prof. Subir K. Das, Prof. Kavita Jain, Prof. S. Balasubramanian, Prof. A. Sundaresan, Prof. C. Narayana, Prof. K. S. Narayan, Prof. R. Ganapathy, Dr. Bivas Saha, Prof. R. Datta, Prof. T. K. Maji, Prof. M. Eswaramoorthy, Prof. Sarit Agasti, Prof. Sridhar Rajaram, Prof. A. Chakraborty (IISc), Dr. Premkumar Senguttuvan, and Prof. N. S. Vidhyadiraja for offering wonderful courses in JNC and the classes during their coursework have greatly helped me in my research.

Its my pleasure to thank my lab-mates, Anirudha, Vinayak, Gurshid, Sujan, Gunjan, Gaur, for all our scientific discussions and making the lab environment pleasant and suitable for research.

My heartfelt thanks to my dear good friends, Dipanjana, Surabhi, Uttam, Animesh, Tarak, Anustup, Amit, Aditya, Vinay, Sohini, and Arif for making my life enjoyable

outside the lab.

Last but not the least, I wish to thank my parents and brother above all, because without their constant encouragement and loving support any study would not have been possible.

Synopsis

Excitation of a metal by ultrashort laser pulse involves very complex processes including electron-electron, electron-photon, electron-phonon, and phonon-phonon scatterings. The ultrafast pulse laser excited solid leads to a nonequilibrium state within the electron and phonon subsystem due to the fact that mainly electrons absorb laser energy and lattice remains cold initially and with the passage of time, two main processes occur:(1) The electrons thermalize due to electron-electron interaction, and (2) The electrons transfer energy to phonons via electron-phonon coupling. Ultrafast relaxation dynamics generally range from nanoseconds to femtoseconds. So, we can ask one important question: what physics we can obtain from a study of the ultrafast relaxation dynamics? Therefore, we explore an answer to this question by studying the electron and phonon thermalization in simple metals excited by a laser pulse and this dissertation is primarily focused on the modelling of the relaxation dynamics of carriers in simple metals excited by a laser pulse, and the role of electron-phonon and phonon-phonon scattering in thermalization.

This thesis consists of three chapters. Chapter 1 provides a brief introduction to Ultrafast spectroscopy and some commonly applied theoretical models which describe the energy relaxation of electrons and phonons after laser irradiation including TTM(two-temperature) model and NEP(nonequilibrium electron and phonon) model. Chapter 2 discusses the NEP(nonequilibrium electron and phonon) model in depth and the motivation behind the implementation of this particular model. We then describe and simplify some of the analytical calculation for this model as it is already done by Shota

Ono. Chapter 3 discusses the findings from the study of nonequilibrium model. In particular we reproduce relaxation dynamics of carriers and the evolution of electrons and phonons distribution function obtained by Shota Ono already. From our study, we find that electrons get thermalized in few femtoseconds (fs) and phonons takes few picoseconds (ps) to come to equilibrium. Therefore, we can describe the electrons temporal evolution of distribution function using a high-temperature effective model but for phonons due to their large relaxation time, we need the full non-equilibrium distribution function analysis. Also, we have studied the time evolution of electrons and phonons distribution function upto 300 - 400 fs. But to understand the phonons relaxation dynamics, we need to go upto 10's of picoseconds. Therefore, our next goal is to parallelize the code for more efficient computation and study complete thermalization in metals.

List of Figures

List of Tables

Contents

Chapter 1

Introduction

1.1 Ultrafast Spectroscopy

Spectroscopy is the study of the interaction between light and matter as a function of wavelength and frequency of the electromagnetic radiation. The time scales of some fundamental interactions are shown in Fig. 1.1. As mentioned in the figure, various important interactions occur in either sub-picoseconds or femtoseconds time scales. Therefore, we need a camera with very high temporal resolution to track the extremely fast interactions, and the ultrafast laser provides such a potential [8]. At present, even the table-top laser source can provide the laser of $\sim$ femtoseconds (fs) pulse duration, and state-of-art laser source can even generate pulses in attoseconds or even sub-attoseconds time scale. Research based on attosecond pulse generation is being heavily investigated recently.

Many important processes in atoms and molecules, as well as the interactions among them, occurs faster than even a time scale of picosecond (1 ps = 10^{-12} s). By the Uncertainty principle, the product of the pulse-duration and the optical bandwidth must be of the order unity (or larger). As the pulse duration increases, the bandwidth decreases correspondingly.

Therefore, due to the Uncertainty principle, a temporally short pulse should have

a broad bandwidth (e.g., a 50-fs pulse gives a bandwidth of about 5 terahertz). A Terahertz radiation generally falls in the frequency range of 0.1 - 10 THz (10^{12} cycles per second). As shown in Fig. 1.2, THz region lies between infrared radiation and microwave radiation, is resistant to the techniques commonly applied in these neighbouring bands [1].

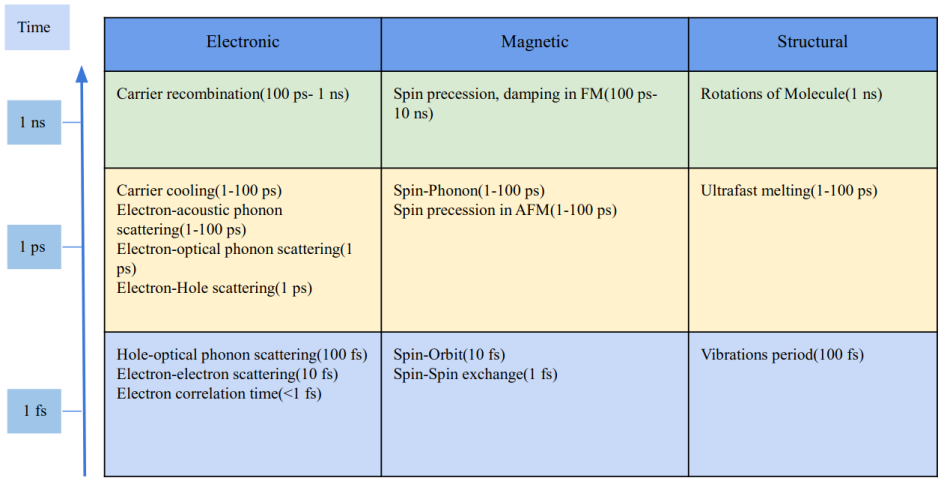

Figure 1.1: Typical time scales of some of the important fundamental interactions.

Therefore, the terahertz (THz) radiation regime of the electromagnetic spectrum is one of the most difficult region to understand since this region shows many common properties with the neighbouring bands. The coherent length of a broad bandwidth radiation is very small which makes ultrashort pulses very useful in bio-imaging applications as well[9].

The ultrafast laser pulses have very high peak power. In the early 1990s, ultrafast laser sources used to produce peak output power of the order of megawatt (10^6 W) in a pulse, directly by a simple laser source. But, for many experiments, a peak power of megawatt is not sufficient which makes it important and necessary to increase the energy of pulse by using amplifier system. Therefore over the past decade, the technology to produce high peak power amplified ultrafast pulses has been progressed rapidly. Due to the high peak power, the ultrafast laser pulse can excite the sample to a non-equilibrium state almost without delay. Such a fast phenomenon gives us a

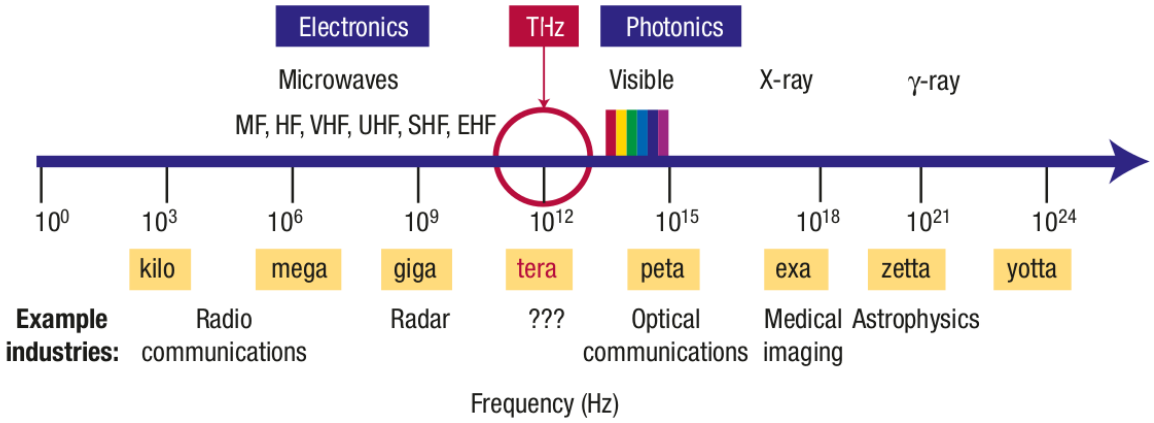

Figure 1.2: The electromagnetic spectrum. This figure is taken from [1]

chance to study the nonequilibrium dynamics far beyond the conventional thermal-equilibrium(or quasiequilibrium) picture.

The ultrafast spectroscopy is a very efficient method to trace the dynamical changes in materials by using the sequences of ultrafast laser pulses. In the last few decades, this field of research is continuously undergoing an exceptional growth in the generation and development of some sophisticated spectroscopy techniques e.g. pump-probe spectroscopy, ultrafast luminescence, and Terahertz spectroscopy. It has become a very powerful tool to understand the basic physical interactions and investigating the unconventional physical phenomena in many newly founded materials.

Typically the third order optical response is monitored using ultrafast spectroscopy experiments for the systems interacting with the sequences of ultrafast light pulses. As shown in Fig. 1.3(a) a system is irradiated by three time-delayed and synchronised light pulses. In the pump-probe spectroscopy, the first two interactions of the pulse field occur with the pump pulse so that t_1=0 and the probe pulse is non-collinear with the pump pulse and generates the nonlinear field in the probe pulse direction (see Fig. 1.3(b)). Therefore by changing the delay between pump and probe pulses enable us to observe the population dynamics of the system [2]. Although very simple conceptually, transient absorption(pump-probe) spectroscopy is very powerful method which has huge applications in solid-state research.

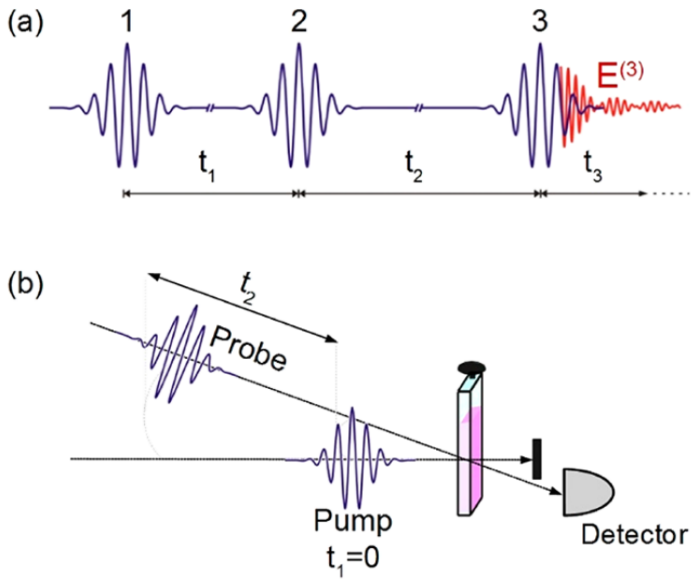

Figure 1.3: (a) General arrangement of a third-order time-resolved nonlinear optical experiment. (b) Pulse sequence in a pump-probe experiment. This figure has been taken from [2]

Nowadays as modern electronics shrink into nano-scale and operate with higher power consumption, thermal management in devices has become an important issue and has drawn attention among the research community in both experimental and theoretical areas[10]. The interplay between different types of scattering have been the object of extensive research for the last two decades both experimentally and theoretically[11]. Many theoretical approaches which investigate the laser induced response of materials, are currently applied on a wide range of time scales. However, the more profound understanding of the ultrafast dynamics of the excitations in solids or the thermalization of carriers even in simple metals is not well understood[6]. During the laser excitation processes, electrons are accelerated by the laser pulse via light-matter interaction and thermalize within femtoseconds to picoseconds and leave ions in their initial state. If the initial state is a solid, then due to electron-phonon energy transfer lattice is heated to a new thermal equilibrium over several picoseconds[12]. Laser excitation of metal with an ultrafast laser pulse pushes the electrons out of equilibrium and to describe this nonequilibrium phenomenon theoretically has become a great interest for many scientists in the last two decade[13].

In thermodynamics, temperature is defined at local thermal equilibrium locations. A local thermal equilibrium means there is a common temperature that can be applied to all the phonon branches and electrons separately. So, in local thermal equilibrium, electrons which are fermions, follow Fermi-Dirac distribution function:

$$f(\epsilon) = \frac{1}{\exp[(\epsilon - \mu)/(k_B T)] + 1} \tag{1.1}$$

where ϵ is the electron energy state, k_B is the Boltzmann constant, and T is the temperature. Phonons which are Bosons and the particle representation of mechanical waves in solids, follow Bose-Einstein distribution:

$$n(\omega) = \frac{1}{\exp[(\hbar\omega)/(k_B T)] - 1} \tag{1.2}$$

where ω is the phonon frequency. On the other hand, thermal nonequilibrium transport involves thermal states which are not in equilibrium and can not be described by Eq.(1.1) and Eq.(1.2). All the materials have multiple branches. Mostly metals with face-centered cubic structure have 3 acoustic phonon branches. Phonons which belongs to different phonon modes generally have different physical properties accordingly. Therefore, under certain conditions, electrons and different phonon branches in the materials can be driven into nonequilibrium regime [10]. Therefore, during the ultrafast laser heating processes, the amount of energy received by different phonons of different phonon modes vary from the electrons due to different *e-ph* coupling strength and as shown in Fig. 1.4, they will not have a common temperature [3]. Therefore, if local thermal equilibrium(quasiequilibrium) is considered, then one may get very inaccurate results or even wrong results and to predict accurate physics behind this phenomenon, the fundamental understanding of the nonequilibrium thermal transport is very necessary. While experiments are a solid approach to describe this highly out-of-equilibrium phenomenon, they have certain limitations. It is extremely difficult to measure direct temperature of electrons and individual phonons branches, which makes

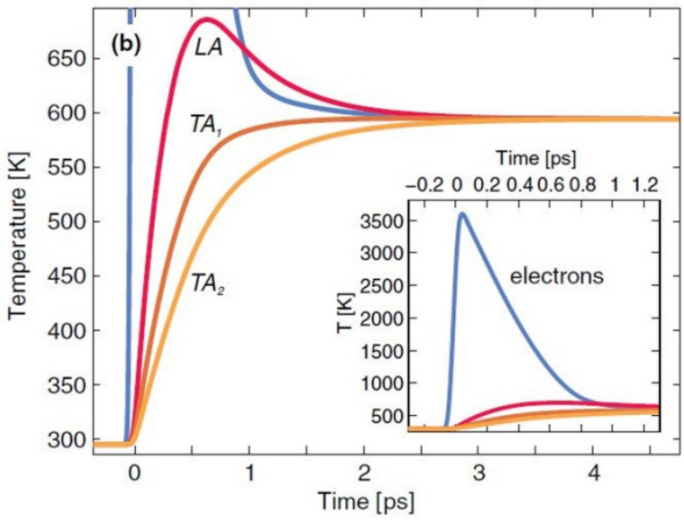

Figure 1.4: Evolution of the temperatures of electrons(blue) and the three phonon branches of Al. This figure has been taken from [3]

this approach not very useful in describing the complete picture of non-equilibrium thermal transport using experiments alone.

Therefore, from a theoretical perspective, nowadays many models (see Fig. 1.5) are commonly applied to describe the ultrafast carrier dynamics in laser excited met-

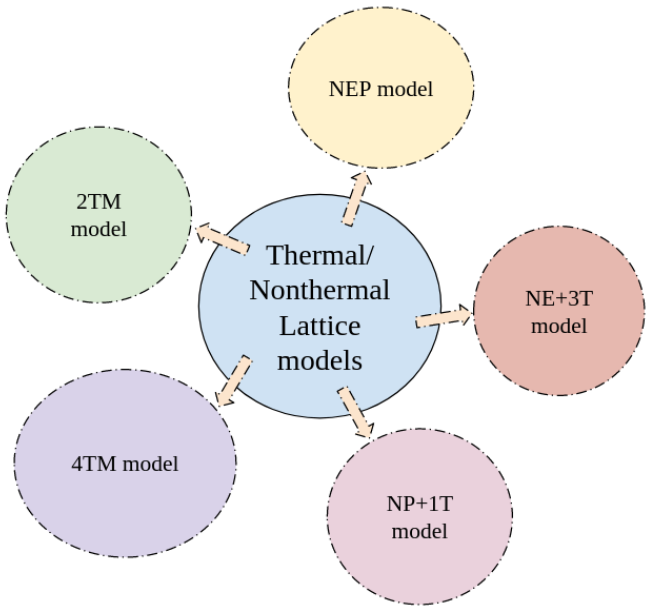

Figure 1.5: Different possibilities of thermal/nonthermal lattice models.

als which are employed in the range of quasiequilibrium to complete non-equilibrium thermal transport.

Fig. 1.5 represents:

- The quasiequilibrium electrons and the quasiequilibrium phonons characterized by one phonon temperature (2TM) model
- The nonequilibrium electrons and the nonequilibrium phonons model (NEP)
- The nonequilibrium electrons and the quasiequilibrium phonons characterized by three phonon temperatures (NE+3T) model
- The nonequilibrium phonons and the quasiequilibrium electrons (NP+1T) model
- The quasiequilibrium electrons and the quasiequilibrium phonons characterized by three phonon temperatures (4TM) model

Notably among these models, the Two-Temperature model (TTM) and Nonequilibrium(NEP) model are the preferred models.

1.2 Two-Temperature model

The thermalization in pump pulse excited solids is governed by many relevant scattering mechanism such as electron-electron (e-e), electron-phonon(e-ph), and phonon-phonon (ph-ph) scattering. In 1957, the energy transfer between electrons and phonons was studied by Kaganov *et al.*[14] via e-ph, and ph-e scattering, which was motivated by the electron transport experiment. Anisimov *et al.*[15] was the first person to apply the Two-Temperature model(2TM) to study the energy relaxation in photoexcited solids. In the framework of 2TM, Allen *et al.*[16] derived a formula ($\gamma_T = 3\hbar\lambda < \omega^2 > /\pi k_B T$) to determine the thermal relaxation rate, which revealed the interplay between the e-ph coupling function used in the Two-temperature model and the Eliashberg function and is widely used in the theory of superconductivity. Later on, Allen's formula was also verified by the ultrafast pulse laser experiments and found to be a fundamental

formula for many traditional metals. Allen pointed out that until the system reaches to thermally equilibrium state, excess electron energy is transferred to the phonon system via e-ph coupling. This idea can be derived from Bloch-Boltzmann-Peierls formulas for the electron and phonon distribution functions:

$$\left[\frac{\partial F_k}{\partial t}\right]_{e-ph} = -\frac{2\pi}{\hbar N_c}\sum_Q |M_{kk'}|^2\{F_k(1-F_{k'})[(N_q+1)\delta(\epsilon_k-\epsilon_{k'}-\hbar\omega_Q)+N_Q\delta(\epsilon_k-\epsilon_{k'}+\hbar\omega_Q)] - (1-F_k)F_{k'}[(N_Q+1)\delta(\epsilon_k-\epsilon_{k'}+\hbar\omega_Q)+N_Q\delta(\epsilon_k-\epsilon_{k'}-\hbar\omega_Q)]\} \tag{1.3}$$

$$\left[\frac{\partial N_Q}{\partial t}\right]_{ph-e} = -\frac{4\pi}{\hbar N_c}\sum_k |M_{kk'}|^2 F_k(1-F_{k'})[N_Q\delta(\epsilon_k-\epsilon_{k'}+\hbar\omega_Q)-(N_Q+1)\delta(\epsilon_k-\epsilon_{k'}-\hbar\omega_Q)] \tag{1.4}$$

The assumptions used in this model were: (a) The electron-electron (coulomb) and phonon-phonon (anharmonic) collision rates are large enough to restrict the electron and phonon distribution function equal to local equilibrium distributions (quasiequilibrium) [17]; (b) Electron-phonon (e-ph) coupling strength between electrons and different branches of acoustic phonons is same, which means all the phonon branches are at same temperature and these electron and phonon quasiequilibrium states are characterized by separate effective electron and phonon temperature T_e and T_{ph} respectively, at any time (see Fig. 1.6); (c) The laser pulse disappears at t=0 leaving electron temperature at an elevated temperature $T_e(0)$; (d) The electrons and phonons are in a thermal quasiequilibrium (QE) with two different time-dependent temperature $T_e(t)$ and $T_{ph}(t)$[18]. The time evolution of the two subsystems can then be described by the time dependence of T_e and T_{ph} derived from the following coupled differential equations[19]:

$$C_e(T_e)\frac{\partial T_e}{\partial t} = -\,G_{e-ph}(T_e - T_{ph}) + P(t)$$
$$C_{ph}(T_{ph})\frac{\partial T_{ph}}{\partial t} = +\,G_{e-ph}(T_e - T_{ph}) \tag{1.5}$$

where C_e and C_{ph} are the heat capacities of electron and phonon, G_{e-ph} the e-ph

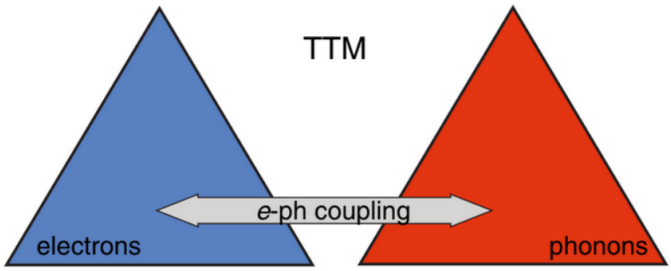

Figure 1.6: Schematic illustration of the Two-Temperature model (2TM). This figure has been taken from [4]

coupling constant, and P(t) represents the absorbed power from laser irradiation.

This idea provides the simplest and intuitive description of the thermalization of electronic and vibrational degrees of freedom in systems out of equilibrium. Also the thermal relaxation rate γ_T has been proved to be proportional to the e-ph coupling factor $\lambda < \omega^2 >$. The factor $\lambda < \omega^2 >$ is of great interest in estimating the superconducting transition transition temperature T_c of metals. However, on below a few hundreds of femtoseconds time scales, electrons distribution can not be defined by thermal quasi-equilibrium distribution function since the nonequilibrium of electrons may come into play. When the system size is so small that it becomes comparable with the energy carrier's mean free path (MFP), electrons and phonons travel almost without scattering with each other. As a result, temperature cannot be defined using Eq. 1.5.

However, the assumption behind 2TM model is questionable in the sense that e-e(coulomb) and ph-ph(anharmonic) scattering rates are not always large enough to keep electron and phonon distribution function equal to local thermal equilibrium. In fact, several experimental and theoretical works based on Boltzmann equation (BOE)

considering all types of possible scatterings have shown the breakdown of the two-temperature model (2TM) in layered materials [17, 20] and even in Aluminium (Al)[3] because in these solids the occupation number of longitudinal phonons (LA) and transverse phonons (TA) are described by Bose-Einstein (BE) distribution function with different temperature, while in the two-temperature model (2TM), these are described by the common temperature. Furthermore, for the better understanding of thermalization in metals, recent studies have revealed the importance and necessity of ph-ph scattering and therefore, a nonequilibrium approximation should now be reconsidered for the thermalization in solids which is nonequilibrium electrons and phonons model (NEP)[21].

1.3 Nonequilibrium electron-phonon (NEP) model

In ultrafast dynamics irradiated by pump pulse laser, nonthermalized electrons have finite relaxation time which means that before the electron subsystem reaches to thermal equilibrium, electrons have transferred energy to phonon subsystem [22]. In this thesis, we investigate the electron and phonon thermalization in the conventional metals by solving the Boltzmann equation (BOE) considering the e-e, e-ph, ph-e, and ph-ph scatterings. Fann *et al.* in [23] has shown that nonthermalized electrons make e-ph relaxation process slower. Also, the coupling constant between electrons and different phonon branches are different and thus temporal nonequilibrium occurs between different phonon modes. Generally in metals, in the initial stage of relaxation, free electrons absorb energy from the laser while the lattice remains cold. Then through the e-ph scattering, most of the electrons energy is transferred into longitudinal acoustic (LA) phonons. Though the e-ph collision time (τ_{e-ph}) may be very much comparable to e-e collision time (τ_{e-e}), the energy transfer from the hot electrons to the cold lattice lasts much longer than the thermalization of the electrons due to the large mass difference between electrons and phonons; which is typically a few tens of picoseconds [24].

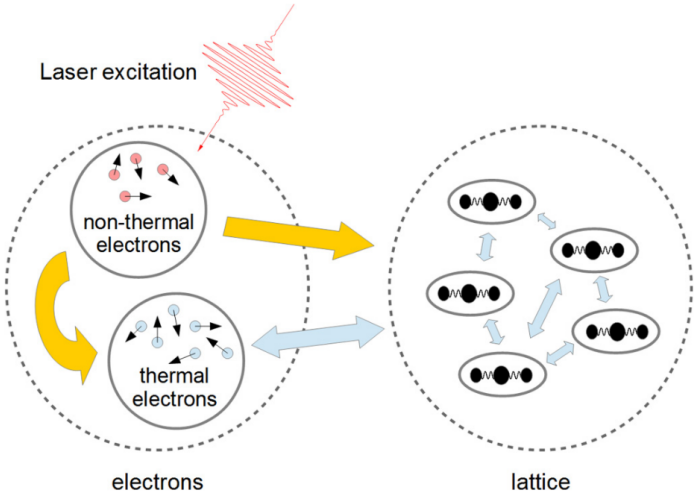

Figure 1.7: Schematic illustration of treating out-of-equilibrium dynamics of electrons and phonons. This figure has been taken from [5]

Simultaneously, via ph-ph scattering, longitudinal acoustic (LA) phonons decay into transverse acoustic (TA) phonons.

We can understand the nonequilibrium scheme of the time evolution of electrons and phonons distribution from Fig. 1.7. So, we can see that the electrons subsystem is initially irradiated by femtosecond laser pulses. A small part that absorbs most of the pulse energy is in nonthermal state whereas the remaining part of the electronic subsystem is considered to be in the local thermal equilibrium[5]. The electronic subsystem then thermalizes by interacting with different phonon subsystem which finally relax their energies by interacting among themselves (depicted by arrows). We can study this nonequilibrium model by solving Boltzmann equation (BOE) without spatial dependence for electron and phonon subsystem where collision integrals consider e-e, e-ph, ph-e, ph-ph scattering, which is written as:

$$\frac{\partial f_{\vec{k},\sigma}}{\partial t} = \Gamma_{e-e} + \Gamma_{e-ph} \tag{1.6}$$

$$\frac{\partial n_{\vec{Q},\gamma}}{\partial t} = \Gamma_{ph-e} + \Gamma_{ph-ph} \tag{1.7}$$

where $f_{\vec{k},\sigma}$ is the distribution of electrons with momentum $\vec{k}$ and $n_{\vec{Q},\gamma}$ the distribution of phonons with momentum $\vec{Q}$. The terms Γ_{x-y} represent complete collision integrals and describe collisions of particles x with particles y[11]. So, Γ_{e-ph} and Γ_{ph-e} represent the collisions between electrons and phonons due to e-ph coupling, Γ_{e-e} describes the collisions between electrons, and Γ_{ph-ph} represents the collisions between phonons[25]. One assumption we have made here is that the external field caused by the laser pulse has vanished at t = 0 and we can neglect the contribution from the diffusion and external field. Therefore a key to the relaxation between laser excited electron bath and the phonons is only scattering term[19]. Generally the applicability of Boltzmann equation (BOE) in metals is restricted by two inequalities:

- $k_f \gg 1/d$ where k_f is the Fermi wave vector and d is the characteristic length of the inhomogeneity of the distribution function and in most cases, d can be tuned with the thickness of the film or the penetration depth of light.
- $\frac{\hbar}{\tau} \ll E_f$ where E_f is the Fermi energy and τ is the characteristic time scale of the changes of the distribution function.

Therefore the application of the Boltzmann equation (BOE) for the description of the time-resolved experiments in the metals is justified on $t > \hbar/E_f$ time scale which is well below the time resolution of all known experiments[26].

Chapter 2

Theoretical Formalism

2.1 NEP Model

NEP model is the nonequilibrium electron and phonon model, with relevant scattering processes. A deeper understanding of the nonequilibrium dynamics of electrons and phonons is very important since it underpin many naturally occurring phenomena e.g. photoluminescence, phase changes, catalysis, and heat transport etc[27]. Though it is very difficult to understand the out-of-equilibrium behavior of carriers, kinetic models such as Boltzmann equation (BOE), allow us to track the evolution of electronic and phononic nonequilibrium. In many investigations published so far, different approaches are used to model the nonequilibrium dynamics of carriers in metals photoexcited with ultrafast laser pulse, where the electron distribution is significantly disturbed but doesn't cause the lattice damage. Here, we use a microscopic out-of-equilibrium dynamics model derived by Shota Ono[6] to laser induced dynamics of electronic and phononic subsystems on subpicoseconds to femtoseconds time scale. In this model, we investigate the electrons and phonons dynamics in the thermalization process in simple metals by solving Boltzmann equation (BOE) which is governed by the electron-electron (e-e), electron-phonon (e-ph), phonon-electron (ph-e), and phonon-phonon (ph-ph) scattering. The relaxation time of electrons and phonons is also substantially influenced by

their initial distribution functions and initial energies, according to research [6].

2.1.1 Hamiltonian

The total Hamiltonian for electrons, phonons, and electron-phonon interaction is written as:

$$\mathcal{H} = \mathcal{H}_e + \mathcal{H}_{ph} + \mathcal{H}_{e-ph} \tag{2.1}$$

where $\mathcal{H}_e$, $\mathcal{H}_{ph}$, and $\mathcal{H}_{e-ph}$ represents the electron, phonon, and electron-phonon interaction Hamiltonian respectively.

- $\mathcal{H}_e$ includes e-e interaction
- $\mathcal{H}_{ph}$ includes ph-ph interaction
- $\mathcal{H}_{e-ph}$ includes e-ph and ph-e interaction part

The expression for each Hamiltonian is given as:

2.1.1.1 Electrons

If we don't neglect the interactions between electrons, then electron-electron collisions, which are not contained in the study of free Fermi gas, can indeed perturb the stationary Bloch states[28]. Now since coulomb interaction is the cause of e-e scatterings, the electron Hamiltonian can be written as:

$$\mathcal{H}_{total}(e) = \mathcal{H}_0 + V_{int}$$

where

$$\mathcal{H}_0 = \sum_{\sigma} \int d\mathbf{r} \Psi_{\sigma}^{+}(\mathbf{r}) h(\mathbf{r}) \Psi_{\sigma}(\mathbf{r})$$

and h($\mathbf{r}$) represents Kinetic Energy part. Similarly,

$$V_{int} = \frac{1}{2}\sum_{\sigma_1\sigma_2}\int d\mathbf{r}_1 d\mathbf{r}_2 \Psi^+_{\sigma_1}(\mathbf{r}_1)\Psi^+_{\sigma_2}(\mathbf{r}_2)v(\mathbf{r}_1,\mathbf{r}_2)\Psi_{\sigma_2}(\mathbf{r}_2)\Psi_{\sigma_1}(\mathbf{r}_1)$$

Therefore,

$$\mathcal{H}_e = \sum_{\sigma}\int d\mathbf{r}\Psi^+_{\sigma}(\mathbf{r})\left(\frac{-\hbar^2}{2m}\nabla^2\right)\Psi_{\sigma}(\mathbf{r}) + \frac{1}{2}\sum_{\sigma\sigma'}\int d\mathbf{r}\int d\mathbf{r}'\Psi^+_{\sigma}(\mathbf{r})\Psi^+_{\sigma'}(\mathbf{r}')v(|\mathbf{x}|)$$
$$\Psi_{\sigma'}(\mathbf{r}')\Psi_{\sigma}(\mathbf{r}) \tag{2.2}$$

where $\hbar$ is the Planck constant, m is the electron mass, and $\mathbf{x}$=$\mathbf{r}$-$\mathbf{r}$'. $\Psi_\sigma(\mathbf{r})$ is the field operator and is given by the expression:

$$\begin{aligned}\Psi_{\sigma}(\mathbf{r}) =& \frac{1}{\sqrt{V}}\sum_{\mathbf{k}} e^{i\mathbf{k}.\mathbf{r}}c_{\mathbf{k}\sigma}\\ \Psi^+_{\sigma}(\mathbf{r}) =& \frac{1}{\sqrt{V}}\sum_{\mathbf{k}} e^{-i\mathbf{k}.\mathbf{r}}c^+_{\mathbf{k}\sigma}\end{aligned} \tag{2.3}$$

where $c^+_{\mathbf{k}\sigma}$ ($c_{\mathbf{k}\sigma}$) is the creation (annihilation) operator of the electrons with wave vector $\mathbf{k}$, spin σ, crystal volume V, v(|x|) is the screened Coulomb potential energy, and its expression is given as:

$$v(|\mathbf{x}|) = \frac{e^2}{4\pi\epsilon_0}\frac{e^{-q_{TF}|x|}}{|\mathbf{x}|}$$

where ϵ_0 is the dielectric constant of vacuum, q_{TF} is the Thomas-Fermi wave number, and its expression is given as:

$$q_{TF} = \left(\frac{12}{\pi}\right)^{1/3}\frac{1}{a_0\sqrt{r_s}}$$

where r_s is the dimensionless Wigner-Seitz radius, and a_0 is the Bohr radius. Now from Eq. 2.2 and Eq. 2.3, we get

$$\mathcal{H}_e = \sum_{\mathbf{k}\sigma} \epsilon_k c^+_{\mathbf{k}\sigma} c_{\mathbf{k}\sigma} + \frac{1}{2} \sum_{\mathbf{q}} \sum_{\mathbf{k}\sigma} \sum_{\mathbf{k}'\sigma'} v_{\mathbf{q}} c^+_{\mathbf{k}+\mathbf{q}\sigma} c^+_{\mathbf{k}'-\mathbf{q}\sigma'} c_{\mathbf{k}'\sigma'} c_{\mathbf{k}\sigma} \tag{2.4}$$

where $\epsilon_k = \hbar^2 k^2/(2m)$ is the free electron energy, v_q is the Fourier component of the screened Coulomb potential, and its expression is given as:

$$v_q = \frac{1}{V} \frac{e^2}{(q^2 + q^2_{TF})}$$

Each term in the summation of the second part of Eq. 2.4 represents a scattering process in which two particles in states $|\mathbf{k}\sigma>$ and $|\mathbf{k}'\sigma'>$ are annihilated, and two particles are created in states $|\mathbf{k} + \mathbf{q}\sigma>$ and $|\mathbf{k}' - \mathbf{q}\sigma'>$. The interaction is viewed as a collision in which one particle transfers momentum $\hbar\mathbf{q}$ to the other. The scattering process may be represented pictorially, as shown in Fig. 3.8

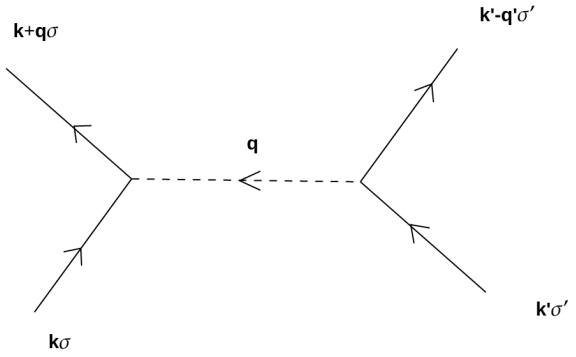

Figure 2.1: Schematic representation of the interaction of two particles.

2.1.1.2 Phonons

We can understand the lattice dynamics in an atomistic system by considering the elastic properties of a crystal which can be viewed as a homogeneous continuum medium rather than as a periodic array of atoms. Generally, the continuum approximation is

valid for elastic waves of wavelengths λ longer than 10^{-6} cm. The total anharmonic Hamiltonian for this system is given by[6]:

$$\mathcal{H}_{total} = \mathcal{H}_2 + \mathcal{H}_3 + \mathcal{O}(4) \tag{2.5}$$

where $\mathcal{H}_2 = T + V_2$ which is harmonic hamiltonian and $\mathcal{H}_3$ is the third order term from the expansion of the crystal potential which is:

$$\mathcal{H}_3 = \frac{1}{3!} \sum_{\substack{ll'l'' \\ kk'k'' \\ \alpha_1\alpha_2\alpha_3}} \psi^{lk,l'k',l''k''}_{\alpha_1\alpha_2\alpha_3} u^{lk}_{\alpha_1} u^{l'k'}_{\alpha_2} u^{l''k''}_{\alpha_3} \tag{2.6}$$

The expression of kinetic energy is given as:

$$T = \frac{1}{2} \sum_{qs} \dot{Q}(\mathbf{q}s)\dot{Q}(-\mathbf{q}s) \tag{2.7}$$

and the expression of the harmonic potential energy is given as:

$$V_2 = \frac{1}{2} \sum_{\mathbf{q}s} \omega^2(\mathbf{q}s) Q(-\mathbf{q}s) Q(\mathbf{q}s) \tag{2.8}$$

such that the harmonic hamiltonian is given by:

$$\mathcal{H}_2 = \frac{1}{2} \sum_{\mathbf{q}s} (P(-\mathbf{q}s)P(\mathbf{q}s) + \omega^2(\mathbf{q}s) Q(-\mathbf{q}s) Q(\mathbf{q}s)) \tag{2.9}$$

In strain tensor notation Eq. 2.5 is written as:

$$\begin{aligned} \mathcal{H}_{total} =& \frac{1}{2\rho_i} \sum_i \int p^*_i(\mathbf{r}) p_i(\mathbf{r}) d\mathbf{r} \\ &+ \frac{1}{2!} \sum_{ijkl} \int d\mathbf{r} C_{ijkl} \eta_{ij}(\mathbf{r}) \eta_{kl}(\mathbf{r}) \\ &+ \frac{1}{3!} \sum_{ijklmn} \int d\mathbf{r} C_{ijklmn} \eta_{ij}(\mathbf{r}) \eta_{kl}(\mathbf{r}) \eta_{mn}(\mathbf{r}) \end{aligned} \tag{2.10}$$

where $C_{ijklmn}(C_{ijkl})$ is the six-rank (fourth-rank) tensor whose expressions are given as:

$$C_{ijkl} = \lambda_L \delta_{ij}\delta_{kl} + \mu_L(\delta_{ik}\delta_{jl} + \delta_{il}\delta_{jk}) \tag{2.11}$$

where λ_L and μ_L are Lame$^{'}e$ constants, while the six-rank tensor is given as:

$$\begin{aligned} C_{ijklmn} =& E_1\delta_{ij}\delta_{kl}\delta_{mn} + E_2[\delta_{ij}(\delta_{km}\delta_{ln} + \delta_{kn}\delta_{lm}) + \delta_{kl}(\delta_{im}\delta_{jn} + \delta_{in}\delta_{jm}) \\ &+ \delta_{mn}(\delta_{ik}\delta_{jl} + \delta_{il}\delta_{jk})] + E_3[\delta_{ik}(\delta_{jm}\delta_{ln} + \delta_{il}(\delta_{jm}\delta_{kn} + \delta_{jn}\delta_{km}) \\ &+ \delta_{im}(\delta_{jk}\delta_{ln} + \delta_{jl}\delta_{kn} + \delta_{in}(\delta_{jk}\delta_{lm} + \delta_{jl}\delta_{km}))] \end{aligned} \tag{2.12}$$

where E_1, E_2, and E_3 are third-order elastic constants, and the strain tensor is defined as:

$$\eta_{ij}(\mathbf{r}) = \frac{1}{2}\left(\frac{\partial u_i}{\partial x_j} + \frac{\partial u_j}{\partial x_i} + \sum_k \frac{\partial u_k}{\partial x_i}\frac{\partial u_k}{\partial x_j}\right) \tag{2.13}$$

The displacement vector $u_i(\mathbf{r})$ is written as:

$$u_i(\mathbf{r}) = \sum_{\mathbf{Q},\gamma} \sqrt{\frac{\hbar}{2\rho_i \Omega \omega_\gamma(\mathbf{Q})}}(b_{\mathbf{Q}\gamma} + b^+_{-\mathbf{Q}\gamma}) \times e_i(\mathbf{Q}\gamma)e^{i\mathbf{Q}.\mathbf{r}} \tag{2.14}$$

where $b_{\mathbf{Q}\gamma}$ and $b^+_{\mathbf{Q}\gamma}$ are the annihilation and creation operators resp. for the phonons with the wave vector $\mathbf{Q}$=(Q_1, Q_2, Q_3) and γ is the polarization which can be LA, TA1, or TA2. $\mathbf{e}(\mathbf{Q}, \gamma)$ is the polarization vector, and the momentum operator in Eq. 2.10 is written as:

$$p_i(\mathbf{r}) = -i \sum_{\mathbf{Q},\gamma} \sqrt{\frac{\hbar \rho_i \omega_\gamma(\mathbf{Q})}{2\Omega}} (b_{\mathbf{Q}\gamma} - b^+_{-\mathbf{Q}\gamma}) \times e_i(\mathbf{Q}\gamma) e^{i\mathbf{Q}.\mathbf{r}} \tag{2.15}$$

Now we can use the orthonormality relation of the polarization vectors for a given $\mathbf{Q}$ which gives:

$$\mathbf{e}^*(\mathbf{Q},\gamma').\mathbf{e}(\mathbf{Q},\gamma) = \delta_{\gamma,\gamma'}$$

and elastic wave equation is given by

$$\rho_i \omega^2_\gamma(\mathbf{Q}) e_i(\mathbf{Q},\gamma) = \sum_k \left(\sum_{jl} C_{ijkl} \mathbf{Q}_j \mathbf{Q}_l \right) e_k(\mathbf{Q},\gamma) \tag{2.16}$$

where ρ_i is the ion mass density such that $\rho_i = M_i N_i/\Omega$ with ion mass M_i and the number of ions N_i in a volume Ω.
In the isotropic approximation, first term of RHS of Eq. 2.16 can be modified as:

$$\begin{aligned}\sum_{jl} C_{ijkl} Q_j Q_l =& C_{i1k1}Q_1Q_1 + C_{i1k2}Q_1Q_2 + C_{i1k3}Q_1Q_3 + C_{i2k1}Q_2Q_1 + C_{i2k2}Q_2Q_2 \\ &+ C_{i2k3}Q_2Q_3 + C_{i3k1}Q_3Q_1 + C_{i3k2}Q_3Q_2 + C_{i3k3}Q_3Q_3\end{aligned}$$

Thus, RHS of Eq. (2.16) can be expanded as:

$$\sum_k \left(\sum_{j,l} C_{ijkl} Q_j Q_l \right) e_k(\mathbf{Q},\gamma) = \Big\{ C_{i111}Q_1Q_1 + C_{i112}Q_1Q_2 + C_{i113}Q_1Q_3 + C_{i211}Q_2Q_1 + C_{i212}Q_2Q_2 + C_{i213}Q_2Q_3 + C_{i311}Q_3Q_1 + C_{i312}Q_3Q_2 + C_{i313}Q_3Q_3 \Big\} e_1(\mathbf{Q},\gamma) + \Big\{ C_{i121}Q_1Q_1 + C_{i122}Q_1Q_2 + C_{i123}Q_1Q_3 + C_{i221}Q_2Q_1 + C_{i222}Q_2Q_2 + C_{i223}Q_2Q_3 + C_{i321}Q_3Q_1 + C_{i322}Q_3Q_2 + C_{i323}Q_3Q_3 \Big\} e_2(\mathbf{Q},\gamma) + \Big\{ C_{i131}Q_1Q_1 + C_{i132}Q_1Q_2 + C_{i133}Q_1Q_3 + C_{i231}Q_2Q_1 + C_{i232}Q_2Q_2 + C_{i233}Q_2Q_3 + C_{i331}Q_3Q_1 + C_{i332}Q_3Q_2 + C_{i333}Q_3Q_3 \Big\} e_3(\mathbf{Q},\gamma) \tag{2.17}$$

Now since

$$C_{ijkl} = \lambda_L \delta_{ij}\delta_{kl} + \mu_L(\delta_{ik}\delta_{jl} + \delta_{il}\delta_{jk})$$

Therefore if we compare the Eq. 2.11 and Eq. 2.17, we get

i	Non zero coefficients of $e_1(\mathbf{Q},\gamma)$	Non zero coefficients of $e_2(\mathbf{Q},\gamma)$	Non zero coefficients of $e_3(\mathbf{Q},\gamma)$
1	$C_{1111}Q_1^2 = (\lambda_L + 2\mu_L)Q_1^2$ $C_{1212}Q_2^2 = \mu_L Q_2^2$ $C_{1313}Q_3^2 = \mu_L Q_3^2$	$C_{1122}Q_1Q_2 = \lambda_L Q_1Q_2$ $C_{1221}Q_2Q_1 = \mu_L Q_2Q_1$	$C_{1133}Q_1Q_3 = \lambda_L Q_1Q_3$ $C_{1331}Q_3Q_1 = \mu_L Q_3Q_1$
2	$C_{2112}Q_1Q_2 = \mu_L Q_1Q_2$ $C_{2211}Q_2Q_1 = \lambda_L Q_2Q_1$	$C_{2121}Q_1^2 = \mu_L Q_1^2$ $C_{2222}Q_2^2 = (\lambda_L + 2\mu_L)Q_2^2$ $C_{2332}Q_3^2 = \mu_L Q_3^2$	$C_{2233}Q_2Q_3 = \lambda_L Q_2Q_3$ $C_{2332}Q_3Q_2 = \mu_L Q_3Q_2$
3	$C_{3113}Q_1Q_3 = \mu_L Q_1Q_3$ $C_{3311}Q_3Q_1 = \lambda_L Q_3Q_1$	$C_{3223}Q_2Q_3 = \mu_L Q_2Q_3$ $C_{3322}Q_3Q_2 = \lambda_L Q_3Q_2$	$C_{3131}Q_1^2 = \mu_L Q_1^2$ $C_{3232}Q_2^2 = \mu_L Q_2^2$ $C_{3333}Q_3^2 = (\lambda_L + 2\mu_L)Q_3^2$

Table 2.1: Details of the relation between various elastic constants and Lam*é* constants.

Now after comparing the data of Eq. 2.16 and Table 2.1, we get

$$\text{For i} = 1, \quad \rho_i \omega_\gamma^2(\mathbf{Q}) e_1(\mathbf{Q},\gamma) = ((\lambda_L + 2\mu_L)Q_1^2 + \mu_L Q_2^2 + \mu_L Q_3^2) e_1(\mathbf{Q},\gamma) \tag{2.18}$$

$$\text{For i} = 2, \quad \rho_i \omega_\gamma^2(\mathbf{Q}) e_2(\mathbf{Q},\gamma) = (\mu_L Q_1^2 + (\lambda_L + 2\mu_L) Q_2^2 + \mu_L Q_3^2 e_2)(\mathbf{Q},\gamma) \tag{2.19}$$

$$\text{For i} = 3, \quad \rho_i \omega_\gamma^2(\mathbf{Q}) e_3(\mathbf{Q},\gamma) = (\mu_L Q_1^2 + \mu_L Q_3^2 + (\lambda_L + 2\mu_L) Q_3^2 e_3)(\mathbf{Q},\gamma) \tag{2.20}$$

Now Eq.[2.18- 2.20] can also be written as:

$$\rho_i \omega_\gamma^2(\mathbf{Q}) = \begin{bmatrix} \lambda_L + 2\mu_L & \mu_L & \mu_L \\ \mu_L & \lambda_L + 2\mu_L & \mu_L \\ \mu_L & \mu_L & \lambda_L + 2\mu_L \end{bmatrix} \begin{bmatrix} Q_1^2 \\ Q_2^2 \\ Q_3^2 \end{bmatrix}$$

Here γ can be either LA, TA1, or TA2 polarization. So, if we take γ=LA polarization as the first case, then we get:

$$\rho_i \omega_{LA}^2(\mathbf{Q}) e_1(\mathbf{Q}, LA) = (\lambda_L + 2\mu_L) Q_1^2 e_1(\mathbf{Q}, LA) \tag{2.21}$$

$$\rho_i \omega_{LA}^2(\mathbf{Q}) e_2(\mathbf{Q}, LA) = (\lambda_L + 2\mu_L) Q_2^2 e_2(\mathbf{Q}, LA) \tag{2.22}$$

$$\rho_i \omega_{LA}^2(\mathbf{Q}) e_3(\mathbf{Q}, LA) = (\lambda_L + 2\mu_L) Q_3^2 e_3(\mathbf{Q}, LA) \tag{2.23}$$

Now after adding above Eq.[2.18-2.23], we get:

$$\rho_i\omega^2_{LA}(\mathbf{Q})\{e_1(\mathbf{Q},LA)+e_2(\mathbf{Q},LA)+e_3(\mathbf{Q},LA)\} = [(\lambda_L+2\mu_L)Q_1^2 + (\lambda_L+2\mu_L)Q_2^2+(\lambda_L+2\mu_L)Q_3^2]\{e_1(\mathbf{Q},LA)+e_2(\mathbf{Q},LA)+e_3(\mathbf{Q},LA)\}$$

or

$$\begin{aligned}\rho_i\omega^2_{LA}(\mathbf{Q}) =&(\lambda_L+2\mu_L)(Q_1^2+Q_2^2+Q_3^2)\\ =&(\lambda_L+2\mu_L)|\mathbf{Q}|^2\end{aligned}$$

which gives

$$\begin{aligned}\omega^2_{LA}(\mathbf{Q}) =&\frac{(\lambda_L+2\mu_L)|\mathbf{Q}|^2}{\rho_i}\\ =&\sqrt{\frac{(\lambda_L+2\mu_L)}{\rho_i}}|\mathbf{Q}|\end{aligned} \tag{2.24}$$

$\implies$ The frequency of LA branch is given by

$$\omega_{LA}(\mathbf{Q}) = \sqrt{\frac{(\lambda_L+2\mu_L)}{\rho_i}}|\mathbf{Q}| \equiv_{LA} |\mathbf{Q}| \tag{2.25}$$

where v_{LA} is the phonon velocity of LA mode. Similarly, if γ=TA1 or TA2, then the wave vector is in the perpendicular direction of the component of polarization. Therefore after doing the same procedure[1] from Eq.[2.21- 2.25], we get the expression of the frequencies of TA1 and TA2 polarization

$$\omega_{TA1}(\mathbf{Q}) = \omega_{TA2}(\mathbf{Q}) = \sqrt{\frac{\mu_L}{\rho_i}}|\mathbf{Q}| \equiv v_{TA}|\mathbf{Q}| \tag{2.26}$$

where v_{TA} is the common phonon velocity of TA1 and TA2 mode.

[1]The details can be obtained from Appendix A.1

Now if we put the $u_i(\mathbf{r})$, $p_i(\mathbf{r})$ values from Eq.[2.14- 2.15] into Eq. 2.10, we get

$$\mathcal{H}_2 = \sum_{\mathbf{Q}\gamma} \hbar\omega_\gamma(\mathbf{Q}) \left(b^+_{\mathbf{Q}\gamma} b_{\mathbf{Q}\gamma} + \frac{1}{2} \right) \tag{2.27}$$

and

$$\begin{aligned} \mathcal{H}_3 =& \frac{1}{3!} \sum_{\substack{\mathbf{Q},\mathbf{Q}',\mathbf{Q}'' \\ \gamma\gamma'\gamma''}} A^{\gamma,\gamma',\gamma''}_{\mathbf{Q},\mathbf{Q}',\mathbf{Q}''} \times (b_{\mathbf{Q}\gamma} + b^+_{-\mathbf{Q}\gamma})(b_{\mathbf{Q}'\gamma'} + b^+_{-\mathbf{Q}'\gamma'})(b_{\mathbf{Q}''\gamma''} + b^+_{-\mathbf{Q}''\gamma''}) \\ =& \frac{1}{6} \sum_{\substack{\mathbf{Q},\mathbf{Q}',\mathbf{Q}'' \\ \gamma\gamma'\gamma''}} A^{\gamma,\gamma',\gamma''}_{\mathbf{Q},\mathbf{Q}',\mathbf{Q}''} \times B_{\mathbf{Q}\gamma} B_{\mathbf{Q}',\gamma'} B_{\mathbf{Q}''\gamma''} \delta_{\mathbf{Q}+\mathbf{Q}'+\mathbf{Q}'',0} \end{aligned} \tag{2.28}$$

where $B_{\mathbf{Q}\gamma} = b_{\mathbf{Q}\gamma} + b^+_{-\mathbf{Q}\gamma}$. The operators act on the phonon states and thus create or destroy phonons in the respective state. Let $|n_{\mathbf{Q}\gamma}>$ denote the occupation number representation of phonons with wave vector $\mathbf{Q}$ in branch γ. Similarly the operator combinations in Eq. 2.28 act on three-phonon states $|n_{\mathbf{Q}\gamma} n_{\mathbf{Q}'\gamma'} n_{\mathbf{Q}''\gamma''}>$ and according to Eq. 2.28, four three-phonon interacting processes can be deduced, which can be either one phonon give rise to two new phonons, or two phonons coalesce into one new phonon. However due to energy conservation, the simultaneous annihilation or creation of three phonons is not allowed. So, by the selection rules for energy and momentum, the following processes are allowed

$$\begin{aligned} \omega(\mathbf{Q}\gamma) + \omega(\mathbf{Q}'\gamma') &= \omega(\mathbf{Q}''\gamma'') \\ \mathbf{Q} + \mathbf{Q}' &= \mathbf{Q}'' + G \end{aligned} \tag{2.29}$$

and

$$\begin{aligned} \omega(\mathbf{Q}\gamma) &= \omega(\mathbf{Q}'\gamma') + \omega(\mathbf{Q}''\gamma'') \\ \mathbf{Q} + G &= \mathbf{Q}' + \mathbf{Q}'' \end{aligned} \tag{2.30}$$

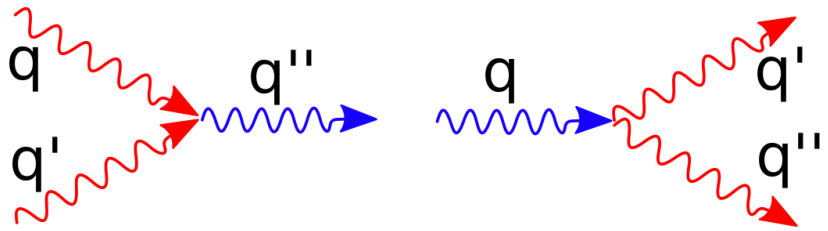

Figure 2.2: Phonons creation and annihilation diagrams

for coalescence and decay of phonons, respectively. These scattering processes are shown in Fig. 2.2. The three-phonon matrix elements $A^{\gamma,\gamma',\gamma''}_{\mathbf{Q},\mathbf{Q}',\mathbf{Q}''}$ in Eq. 2.28 is given by:

$$A^{\gamma,\gamma',\gamma''}_{\mathbf{Q},\mathbf{Q}',\mathbf{Q}''} = -\frac{i}{\sqrt{\Omega}}\left(\frac{\hbar}{2\rho_i}\right)^{3/2}\frac{A_{ph}}{\sqrt{\omega_\gamma(\mathbf{Q})\omega_{\gamma'}(\mathbf{Q}')\omega_{\gamma''}(\mathbf{Q}'')}} \tag{2.31}$$

where ${A_{ph}}^2$ is defined as:

$$\begin{aligned}
A_{ph} = {} & E_1(\mathbf{e}.\mathbf{Q})(\mathbf{e}'.\mathbf{Q}')(\mathbf{e}''.\mathbf{Q}'') + E_2(\mathbf{e}.\mathbf{Q})[(\mathbf{e}'.\mathbf{e}'')(\mathbf{Q}',\mathbf{Q}'') + (\mathbf{e}'.\mathbf{Q}'')(\mathbf{e}''.\mathbf{Q}')] + E_2(\mathbf{e}'.\mathbf{Q}') \\
& + [(\mathbf{e}.\mathbf{e}'')(\mathbf{Q}.\mathbf{Q}'') + (\mathbf{e}.\mathbf{Q}'')(\mathbf{e}''.\mathbf{Q})] + E_2(\mathbf{e}''.\mathbf{Q}'')[(\mathbf{e}.\mathbf{e}')(\mathbf{Q}.\mathbf{Q}') + (\mathbf{e}.\mathbf{Q}')(\mathbf{e}'.\mathbf{Q})] \\
& + E_3(\mathbf{e}.\mathbf{e}')[(\mathbf{e}''.\mathbf{Q})(\mathbf{Q}'.\mathbf{Q}'') + (\mathbf{Q}.\mathbf{Q}'')(\mathbf{e}''.\mathbf{Q}')] + E_3(\mathbf{e}.\mathbf{Q}')[(\mathbf{e}''.\mathbf{Q})(\mathbf{e}'.\mathbf{Q}'') + (\mathbf{Q}.\mathbf{Q}'') \\
& (\mathbf{e}'.\mathbf{e}'')] + E_3(\mathbf{e}.\mathbf{e}'')[(\mathbf{e}'.\mathbf{Q})(\mathbf{Q}'.\mathbf{Q}'') + (\mathbf{Q}.\mathbf{Q}')(\mathbf{e}'.\mathbf{e}'')] + \lambda_L[(\mathbf{e}.\mathbf{Q})(\mathbf{e}'.\mathbf{e}'')(\mathbf{Q}'.\mathbf{Q}'') + (\mathbf{e}.\mathbf{e}'') \\
& (\mathbf{Q}.\mathbf{Q}'')(\mathbf{e}'.\mathbf{Q}') + (\mathbf{e}.\mathbf{e}')(\mathbf{Q}.\mathbf{Q}')(\mathbf{e}''.\mathbf{Q}'')] + \mu_L[(\mathbf{e}.\mathbf{e}')(\mathbf{Q}.\mathbf{e}'')(\mathbf{Q}'.\mathbf{Q}'') + (\mathbf{e}.\mathbf{e}')(\mathbf{Q}.\mathbf{Q}'') \\
& (\mathbf{Q}'.\mathbf{e}'') + (\mathbf{e}.\mathbf{Q}')(\mathbf{Q}.\mathbf{Q}'')(\mathbf{e}'.\mathbf{e}'') + (\mathbf{e}.\mathbf{e}'')(\mathbf{Q}.\mathbf{e}')(\mathbf{Q}'.\mathbf{Q}'') + (\mathbf{e}.\mathbf{e}'')(\mathbf{Q}.\mathbf{Q}')(\mathbf{e}'.\mathbf{Q}'') + (\mathbf{e}.\mathbf{Q}'') \\
& (\mathbf{Q}.\mathbf{Q}')(\mathbf{e}'.\mathbf{e}'')]
\end{aligned} \tag{2.32}$$

Now γ, γ', and γ'' can be either LA, TA1, or TA2. So, many selection rules are possible for the combination of different phonon modes. From Eq. 2.32, we have found that three dominant decaying processes are possible:

[2]Abbreviation used in this term is: $\mathbf{e}$=$\mathbf{e}(\mathbf{Q}\gamma)$, $\mathbf{e}' = \mathbf{e}(\mathbf{Q}'\gamma')$, $\mathbf{e}'' = \mathbf{e}(\mathbf{Q}''\gamma'')$
A_{ph} is symmetric under the exchanges $(\mathbf{e},\mathbf{Q})\leftrightarrow(\mathbf{e}',\mathbf{Q}')$, $(\mathbf{e}',\mathbf{Q}') \leftrightarrow (\mathbf{e}'',\mathbf{Q}'')$, and $(\mathbf{e},\mathbf{Q})\leftrightarrow(\mathbf{e}'',\mathbf{Q}'')$

$$LA \rightleftharpoons LA + TA1$$
$$LA \rightleftharpoons TA1 + TA1$$
$$LA \rightleftharpoons TA2 + TA2$$

Let us take the first selection rule[3]

$$LA(\mathbf{Q}) \rightleftharpoons LA(\mathbf{Q}') + TA1(\mathbf{Q}'') \tag{2.33}$$

where $\mathbf{Q}'' = (\mathbf{Q} - \mathbf{Q}')$, and let $\mathbf{Q} = Q\hat{k}$, then

$$\mathbf{Q}\mathbf{Q}' = QQ' \cos\theta'$$

Therefore

$$\begin{aligned} \mathbf{Q}''.\hat{k} = Q''.\cos\theta'' &= (\mathbf{Q} - \mathbf{Q}').\hat{k} \\ \implies \cos\theta'' &= \frac{Q - Q'\cos\theta'}{Q''} \end{aligned} \tag{2.34}$$

Similarly

$$\begin{aligned} \mathbf{Q}''.\hat{i} = Q''.\sin\theta''\cos\phi'' &= (\mathbf{Q} - \mathbf{Q}').\hat{i} \\ \implies \sin\theta'' &= -Q'\frac{\sin\theta'\cos\phi'}{Q''\cos\phi''} \end{aligned} \tag{2.35}$$

[3]Phonons wave vector and polarization vector can be expressed using spherical coordinates system and the details for these relations can be obtained from Appendix A.2

and

$$\begin{aligned}\mathbf{Q}''.\hat{j} = Q''.\sin\theta''\sin\phi'' &= (\mathbf{Q}-\mathbf{Q}').\hat{j} \\ \implies \sin\theta'' &= -Q'\frac{\sin\theta'\sin\phi'}{Q''\sin\phi''}\end{aligned} \tag{2.36}$$

Now after comparing Eq. 2.35 and Eq. 2.36, we get

$$\phi' = \phi''$$

Therefore

$$\sin\theta'' = \left(\frac{-Q'}{Q''}\right)\sin\theta'$$

Now let us take the **first** term in Eq. 2.32,

$$\begin{aligned}\hat{\mathbf{e}}.\mathbf{Q} &= Q \\ \hat{\mathbf{e}}'.\mathbf{Q}' &= \hat{\mathbf{e}}_{r'}.Q'\hat{\mathbf{e}}_{r'} = Q' \\ \hat{\mathbf{e}}''.\mathbf{Q}'' &= \mathbf{e}_{\theta''}Q''\mathbf{e}_{r''} = 0\end{aligned}$$

From above equations we can see that the first term will vanish for processes involving the TA phonons irrespective of the selection rule, and therefore we can ignore E_1.
For the **second** term,

$$\begin{aligned}\hat{\mathbf{e}}'.\hat{\mathbf{e}}'' = \hat{\mathbf{e}_{r'}}\hat{\mathbf{e}_{\theta''}} &= \sin\theta'\cos\phi'\cos\theta''\cos\phi'' + \sin\theta'\sin\phi'\cos\theta''\sin\phi'' - \cos\theta'\sin\theta' \\ &= \sin\theta'\cos\theta'' - \cos\theta'\sin\theta'' \\ &= \sin\theta'\left(\frac{Q-Q'\cos\theta'}{Q''}\right) + \sin\theta'\left(\frac{Q'\cos\theta'}{Q''}\right) \\ &= \frac{Q}{Q''}\sin\theta'\end{aligned}$$

$$\begin{aligned}\mathbf{Q}'.\mathbf{Q}'' &= \mathbf{Q}'.(\mathbf{Q}-\mathbf{Q}') \\ &= QQ'\cos\theta' - Q'^2 \\ &= Q'(Q\cos\theta' - Q')\end{aligned}$$

$$\begin{aligned}\hat{\mathbf{e}}'.\mathbf{Q}'' &= \hat{e_r}'.(\mathbf{Q}-\mathbf{Q}') \\ &= Q\cos\theta' - Q'\end{aligned}$$

$$\hat{\mathbf{e}}''.\mathbf{Q}' = \mathbf{e}_{\hat{\theta''}}Q'\mathbf{e}_{\hat{r'}} = \left(\frac{QQ'}{Q''}\right)\sin\theta'$$

Therefore, the second term of Eq. 2.32 is

$$2E_2\left(\frac{QQ'}{Q''}\right)[Q^2\sin\theta'\cos\theta' - QQ'\sin\theta'] \tag{2.37}$$

For the **third** term,

$$\begin{aligned}\hat{\mathbf{e}}.\hat{\mathbf{e}}'' &= -\sin\theta'' = \frac{Q'}{Q''}\sin\theta' \\ \hat{\mathbf{e}}.\mathbf{Q}'' &= Q''\cos\theta'' = Q - Q'\cos\theta' \\ \hat{\mathbf{e}}''.\mathbf{Q} &= \mathbf{e}_{\hat{\theta''}}.Q.\hat{k} = -Q\sin\theta'' = \frac{QQ'}{Q''}\sin\theta' \\ \mathbf{Q}.\mathbf{Q}'' &= \mathbf{Q}.(\mathbf{Q}-\mathbf{Q}') = Q(Q - Q'\cos\theta')\end{aligned}$$

Therefore, the third term of Eq. 2.32 is

$$2E_2\left(\frac{QQ'}{Q''}\right)Q'\sin\theta'(Q - Q'\cos\theta') \tag{2.38}$$

For the **fourth** term,

$$\hat{\mathbf{e}}''.\mathbf{Q}'' = 0 \tag{2.39}$$

For the **fifth** term,

$$\hat{\mathbf{e}}.\hat{\mathbf{e}}' = \hat{\mathbf{e}_r}.\hat{\mathbf{e}_{r'}} = \cos\theta'$$

Therefore, the fifth term of Eq. 2.32 is

$$E_3\left(\frac{QQ'}{Q''}\right)[(Q^2 - Q'^2)\sin\theta'\cos\theta'] \tag{2.40}$$

For the **sixth** term,

$$\hat{\mathbf{e}}'.\mathbf{Q}'' = \hat{\mathbf{e}_{r'}}(Q\hat{k} - Q'\hat{\mathbf{e}_{r'}}) = Q\cos\theta' - Q'$$

Therefore, the sixth term of Eq. 2.32 is

$$E_3\left(\frac{QQ'}{Q''}\right)(Q^2 - Q'^2)\sin\theta'\cos\theta' \tag{2.41}$$

For the **seventh** term,

$$\hat{\mathbf{e}}'.\mathbf{Q} = \hat{\mathbf{e}_{r'}}.\mathbf{Q} = Q\cos\theta'$$

Therefore, the seventh term of Eq. 2.32 is

$$2E_3\left(\frac{QQ'}{Q''}\right)Q'\sin\theta'\cos\theta'(Q\cos\theta' - Q') \tag{2.42}$$

The solution of the **eighth** term is:

$$2E_3\left(\frac{QQ'}{Q''}\right)Q\sin\theta'\cos\theta'(Q - Q'\cos\theta') \tag{2.43}$$

The solution of the **ninth** term is:

$$\lambda_L\left(\frac{QQ'}{Q''}\right)(Q^2 - Q'^2)\sin\theta'\cos\theta' \tag{2.44}$$

The solution of the **tenth** term is:

$$3\mu_L \left(\frac{QQ'}{Q''}\right)(Q^2 - Q'^2)\sin\theta'\cos\theta' \tag{2.45}$$

Therefore, after adding Eq.[2.37- 2.45], we get

$$A_{ph} = \frac{QQ'}{Q''}(2E_2 + 4E_3 + \lambda_L + 3\mu_L)(Q^2 - Q'^2)\sin\theta'\cos\theta' \tag{2.46}$$

Similarly for the second selection rule:

$$LA(\mathbf{Q}) \rightleftharpoons TA1(\mathbf{Q}') + TA1(\mathbf{Q}'') \tag{2.47}$$

The A_{ph} solution[4] for above Eq. 2.47 is given by:

$$A_{ph} = \frac{QQ'}{Q''}[E_2 + \lambda_L + 2(E_3 + \mu_L)](Q' - Q\cos\theta)^2 - (E_2 + 2E_3 + \mu_L)Q^2\sin^2\theta' \tag{2.48}$$

And for the third selection rule:

$$LA(\mathbf{Q}) \rightleftharpoons TA2(\mathbf{Q}') + TA2(\mathbf{Q}'') \tag{2.49}$$

The A_{ph} solution[4] for above Eq. 2.49 is given by:

$$A_{ph} = QQ'[(E_2 + \lambda_L)(Q\cos\theta' - Q') + 2(E_3 + \mu_L)(Q - Q'\cos\theta')\cos\theta'] \tag{2.50}$$

The energy and momentum conservation restricts the allowed splitting processes to only 2.33, 2.47, and 2.49 and the collinear process $LA(\mathbf{Q}) \rightleftharpoons LA(\mathbf{Q}') + LA(\mathbf{Q}'')$. But the contribution to the decay rate by the collinear process has found to be very small compared to other three processes mentioned. Hence, we ignore the collinear process in our calculations.

[4]The details can be obtained from Appendix A.3

2.1.1.3 Electron-phonon interaction

In determining the transport properties of metals, the coupling or interaction between electrons and phonons plays a very important role. The electron-phonon coupling is responsible for several many-body effects, e.g. in the measurements of specific heat at low temperature, the increase in the effective mass of electrons can be observed[29]. The electron-phonon interaction Hamiltonian in second-quantized form is given by

$$\mathcal{H}_{el-ph} = \sum_{\mathbf{k},\mathbf{Q},\sigma,\gamma} g(\mathbf{Q},\gamma) a^{+}_{\mathbf{k}'\sigma} a_{\mathbf{k}\sigma} (b_{\mathbf{Q}\gamma} + b^{+}_{-\mathbf{Q}\gamma}) \tag{2.51}$$

where the operators $b_{\mathbf{Q}\gamma}$ and $b^{+}_{-\mathbf{Q}\gamma}$ are annihilation and creation operators respectively for phonons of wave vectors $\mathbf{Q}$ with branch index γ. The selection rule which connects the Bloch vectors $\mathbf{k}'$ and $\mathbf{k}$ with phonons wave vectors $\mathbf{Q}$ is given by

$$\mathbf{k}' = \mathbf{k} + \mathbf{Q} + \mathbf{G}$$

where $\mathbf{G}$ is the reciprocal lattice vector. And in the above equation, the expression of $g(\mathbf{Q},\gamma)$ is given by[6]:

$$|g(\mathbf{Q},\gamma)|^2 = \mathbf{D}_0^2 \frac{\hbar|\mathbf{Q}|}{2\rho_i \Omega v_{LA}} \delta_{\gamma,LA} \tag{2.52}$$

where $\mathbf{D}_0$ is the deformation potentials, which describes the coupling between the LA phonon and electrons. The free-electron approximation approach shows, $\mathbf{D}_0 = 2\epsilon_f/3$, where ϵ_f denotes the Fermi energy. Eq. 2.52 shows the matrix elements for LA phonon mode only but if we want to consider TA phonon, then there should be one general form of $g(\mathbf{Q},\gamma)$ which is written as:

$$|g(\mathbf{Q},\gamma)|^2 = \mathbf{D}_\gamma^2 \frac{\hbar|\mathbf{Q}|}{2\rho_i \Omega v_\gamma} \tag{2.53}$$

where $D_{TA} = \left(\frac{v_{TA}}{v_{LA}}\right)^{\beta} \mathbf{D}_0$. In our calculation we have taken $\beta = 1.5$

2.2 NEP model: A Boltzmann transport approach

This section involves the calculations in NEP (nonequilibrium electron and phonon) model are based on the semi-classical Boltzmann transport equation which considers the relevant scattering processes. The coupled Boltzmann equation (BOE) for electron and phonon systems without magnetic field expressed as:

$$\frac{\partial f_{\mathbf{k},\sigma}}{\partial t} + \mathbf{v}_e.\nabla_{\mathbf{r}} f_{\mathbf{k},\sigma} - \frac{e\mathbf{E}}{\hbar}.\nabla_{\mathbf{k},\sigma} f_{\mathbf{k},\sigma} = \left(\frac{\partial f}{\partial t}\right)_{e-e} + \left(\frac{\partial f}{\partial t}\right)_{e-ph} \tag{2.54}$$

$$\frac{\partial n_{\mathbf{Q},\gamma}}{\partial t} + \mathbf{v}_{ph,\gamma}.\nabla_{\mathbf{r}} n_{\mathbf{Q},\gamma} = \left(\frac{\partial n}{\partial t}\right)_{ph-e} + \left(\frac{\partial n}{\partial t}\right)_{ph-ph} \tag{2.55}$$

where $f_{\mathbf{k},\sigma}$ denotes the distribution function of electrons and $n_{\mathbf{Q},\gamma}$ denotes the distribution function of phonon subsystem. The right-hand sides denote the e-e, e-ph, ph-e, ph-ph scatterings (collision integrals). If the external field caused by the laser has disappeared at t = 0 ps and we do not consider the influence of transport (diffusion), and external electric field term on the change of phonon-population. These simplified BOE approaches have been widely used in investigating the phononic heat transport[10]. So, within the Boltzmann transport model Eq. 2.54 and Eq. 2.55 can be rewritten as:

$$\frac{\partial f_{\mathbf{k},\sigma}}{\partial t} = \left(\frac{\partial f}{\partial t}\right)_{e-e} + \left(\frac{\partial f}{\partial t}\right)_{e-ph} \tag{2.56}$$

$$\frac{\partial n_{\mathbf{Q},\gamma}}{\partial t} = \left(\frac{\partial n}{\partial t}\right)_{ph-e} + \left(\frac{\partial n}{\partial t}\right)_{ph-ph} \tag{2.57}$$

So, to estimate the transition probability due to a particular scattering mechanism many-body perturbation theory and Fermi's golden rule can be employed.

2.2.1 Electron-electron collisions

The collision integral for the electron-electron (e-e) scattering process is given by[6]:

$$\left(\frac{\partial f}{\partial t}\right)_{e-e} = \sum_{\mathbf{k}',\mathbf{q}} \frac{2\pi}{\hbar}|\tilde{V}(\mathbf{q})|^2\delta(\Delta\epsilon)[-f_{\mathbf{k}}f'_{\mathbf{k}}(1-f_{\mathbf{k}+\mathbf{q}})+(1-f_{\mathbf{k}})(1-f_{\mathbf{k}'})f_{\mathbf{k}+\mathbf{q}}f_{\mathbf{k}'-\mathbf{q}}] \quad (2.58)$$

where $\Delta\epsilon = \epsilon_{\mathbf{k}} + \epsilon'_{\mathbf{k}} - \epsilon_{\mathbf{k}+\mathbf{q}} - \epsilon_{\mathbf{k}'-\mathbf{q}}$ (see Fig. 3.8). The e-e collision process described above is given by $(\mathbf{k},\mathbf{k}') \rightleftharpoons (\mathbf{k}+\mathbf{q},\mathbf{k}'-\mathbf{q})$, and expression of $\tilde{V}(\mathbf{q})$ (screened Coulomb interaction potential) is written as

$$\tilde{V}_{\mathbf{q}} = \frac{1}{V}\frac{e^2}{(q^2+q_{TF}^2)}$$

When $f_{\mathbf{k}}$ is averaged over the electron states having the energy ϵ, the we can obtain the energy distribution function for the electrons which is given by:

$$f(\epsilon) = \frac{1}{\mathcal{N}(\epsilon)}\sum_{\mathbf{k}}\delta(\epsilon-\epsilon_{\mathbf{k}})f_{\mathbf{k}} \quad (2.59)$$

where $\mathcal{N}(\epsilon) = \Omega(2m)^{3/2}\sqrt{\epsilon}/4\pi^2\hbar^3$ is the density of states (DOS) per spin.

2.2.2 Electron-phonon and phonon-electron collisions

The collision integral for the electron-phonon (e-ph) and phonon-electron (ph-e) scattering process is given by[6]:

$$\begin{aligned}\left(\frac{\partial f}{\partial t}\right)_{e-ph} = \sum_{\mathbf{Q},\gamma}\frac{2\pi}{\hbar}|g(\mathbf{Q},\gamma)|^2\{&-f_{\mathbf{k}}(1-f_{\mathbf{k}+\mathbf{Q}})[(1+n_{\mathbf{Q}})\delta(\epsilon_{\mathbf{k}}-\epsilon_{\mathbf{k}+\mathbf{Q}}-\hbar\omega_{\mathbf{Q}\gamma})\\ &+n_{\mathbf{Q}}\delta(\epsilon_{\mathbf{k}}-\epsilon_{\mathbf{k}+\mathbf{Q}}+\hbar\omega_{\mathbf{Q}\gamma})]+(1-f_{\mathbf{k}})f_{\mathbf{k}+\mathbf{Q}}[(1+n_{\mathbf{Q}})\delta(\epsilon_{\mathbf{k}}-\epsilon_{\mathbf{k}+\mathbf{Q}}+\hbar\omega_{\mathbf{Q}\gamma})\\ &+n_{\mathbf{Q}}\delta(\epsilon_{\mathbf{k}}-\epsilon_{\mathbf{k}+\mathbf{Q}}-\hbar\omega_{\mathbf{Q}\gamma})]\}\end{aligned} \quad (2.60)$$

$$\left(\frac{\partial n}{\partial t}\right)_{ph-e} = \sum_{\mathbf{k}} \frac{4\pi}{\hbar}|g(\mathbf{Q},\gamma)|^2 f_{\mathbf{k}}(1-f_{\mathbf{k}+\mathbf{Q}})[-n_{\mathbf{Q},\gamma}\delta(\epsilon_{\mathbf{k}}-\epsilon_{\mathbf{k}+\mathbf{Q}}+\hbar\omega_{\mathbf{Q}\gamma})+(1+n_{\mathbf{Q},\gamma}) \\ \delta(\epsilon_{\mathbf{k}}-\epsilon_{\mathbf{k}+\mathbf{Q}}-\hbar\omega_{\mathbf{Q}\gamma})] \tag{2.61}$$

By emitting or absorbing phonons, excess energy of electrons decreases or increases respectively. Eq. 2.60 and Eq. 2.61 consider scattering processes which involves the absorption or emission of single phonon only[29]. Therefore the processes, which involve the emission or absorption of two or more phonons are of negligible importance here. Eq. 2.60 and Eq. 2.61 describes the electron-phonon (e-ph) and phonon-electron (ph-e) collision integrals, where by an absorption of the phonon with $\mathbf{Q}$, electron with state $\mathbf{k}$ is scattered into a new state $\mathbf{k}+\mathbf{Q}$ or by an emission of the phonon with -$\mathbf{Q}$, and vice-versa. The different emission and absorption processes are illustrated in Fig. 2.3

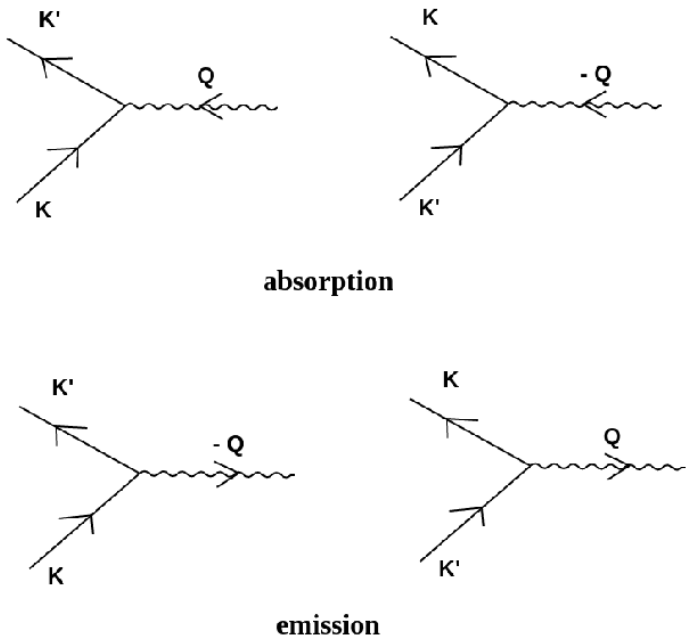

Figure 2.3: Scattering of electrons with emission or absorption of phonons

The expression of $g(\mathbf{Q},\gamma)$ is given by Eq. 2.53, and the phonons energy distribution

function is given by

$$n_\gamma(\omega) = \frac{1}{\mathcal{D}_\gamma(\omega)} \sum_{\mathbf{Q}} \delta(\omega - \omega_{\mathbf{Q}\gamma}) n_{\mathbf{Q},\gamma} \tag{2.62}$$

where ω is the frequency of phonon states. $\mathcal{D}_\gamma$ is the density of states (DOS) of phonons with polarization γ, and the expression of $\mathcal{D}_\gamma$ is defined as

$$\mathcal{D}_\gamma(\omega) = \frac{\Omega\omega^2}{(2\pi^2 v_\gamma^3)} \theta_H(\Omega_{\gamma,D} - \omega)$$

where θ_H is the Heaviside step function with $\theta(x) = 1$ for x ≥ 0 and $\theta(x) = 0$ for x ≤ 0.

2.2.3 Phonon - phonon collisions

The collision integral for the phonon-phonon (ph-ph) scattering process is given by[6]:

$$\begin{aligned}\left(\frac{\partial n}{\partial t}\right)_{ph-ph} = \sum_{\mathbf{Q}'\gamma'\gamma''} \frac{2\pi}{\hbar} |A^{\gamma,\gamma',\gamma''}_{\mathbf{Q},\mathbf{Q}',-(\mathbf{Q}+\mathbf{Q}')}|^2 \Big\{ \frac{1}{2}[(1 + n_{\mathbf{Q},\gamma}) n_{-\mathbf{Q}',\gamma'} n_{\mathbf{Q}+\mathbf{Q}',\gamma''} - n_{\mathbf{Q},\gamma}(1 + n_{-\mathbf{Q}',\gamma'}) \\ (1 + n_{\mathbf{Q}+\mathbf{Q}',\gamma''})] \times \delta(\hbar\omega_{\mathbf{Q},\gamma} - \hbar\omega_{-\mathbf{Q}',\gamma'} - \hbar\omega_{\mathbf{Q}+\mathbf{Q}',\gamma''}) + [(1 + n_{\mathbf{Q},\gamma})(1 + n_{\mathbf{Q}',\gamma'}) \\ n_{\mathbf{Q}+\mathbf{Q}',\gamma''} - n_{\mathbf{Q},\gamma} n_{\mathbf{Q}',\gamma'}(1 + n_{\mathbf{Q}+\mathbf{Q}',\gamma''})] \delta(\hbar\omega_{\mathbf{Q},\gamma} + \hbar\omega_{\mathbf{Q}',\gamma'} - \hbar\omega_{\mathbf{Q}+\mathbf{Q}',\gamma''})\end{aligned} \tag{2.63}$$

$A^{\gamma,\gamma',\gamma''}_{\mathbf{Q},\mathbf{Q}',-(\mathbf{Q}+\mathbf{Q}')}$ is defined in Eq. 2.31, and $\gamma, \gamma', \gamma''$ are restricted with selection rules rules mentioned in Eq.[2.33, 2.47, 2.49]. Again we do not consider the three-phonon collinear processes (in which all three phonons belong to the same phonon branch or polarization) such as LA(TA) $\rightleftharpoons$ LA(TA)+LA(TA), and there are no scattering processes in which one TA phonon creates two LA phonons due to energy conservation law[30]. In Eq. 2.63, the first process describes the decay of one phonon with $(\mathbf{Q}, \gamma)$ into two phonons with $(\mathbf{Q}', \gamma')$ and $(\mathbf{Q} - \mathbf{Q}', \gamma'')$, while for the case of the second process two phonon modes with $(\mathbf{Q}, \gamma)$ and $(\mathbf{Q}', \gamma')$ coalesce into a phonon with $(\mathbf{Q} + \mathbf{Q}', \gamma'')$ [see Fig. 2.2]. Due to the inversion symmetry, the relations $\omega_{\mathbf{Q}\gamma} = \omega_{-\mathbf{Q}\gamma}$ and $n_{\mathbf{Q},\gamma} = n_{-\mathbf{Q},\gamma}$ are used in the derivation of the collision terms (2.63, 2.61, 2.60).

Now after putting all collision integral terms into Eq. 2.56, 2.57, using DOS expression for electrons and phonons, the time (t) evolution for the electron and phonon distribution functions are given by, respectively[6],

$$\begin{aligned}\frac{\partial f(\epsilon)}{\partial t} =& 2\pi \int d\epsilon' \int d\xi \int d\xi' C_{e-e}(\epsilon,\epsilon',\xi,\xi')\delta(\epsilon+\epsilon'-\xi-\xi')\{-f(\epsilon)f(\epsilon')[1-f(\xi)][1-f(\xi')] \\ &+ [1-f(\epsilon)][1-f(\epsilon')]f(\xi)f(\xi')\} + 2\pi \sum_{\gamma} \int d\xi \int d\omega C_{e-ph}(\epsilon,\xi,\omega,\gamma)(\delta(\epsilon-\xi-\hbar\omega) \\ &\{[f(\xi)-f(\epsilon)]n_{\gamma}\omega\} - f(\epsilon)[1-f(\xi)] + \delta(\epsilon-\xi+\hbar\omega)\{[f(\xi)-f(\epsilon)]n_{\gamma}(\omega) + f(\xi) \\ &[1-f(\epsilon)]\}) \end{aligned} \tag{2.64}$$

$$\begin{aligned}\frac{\partial n_{\gamma}(\omega)}{\partial t} =& 4\pi \int d\epsilon \int d\xi C_{ph-e}(\epsilon,\xi,\omega,\gamma)f(\epsilon)[1-f(\xi)]\{-n_{\gamma}(\omega)\delta(\epsilon-\xi+\hbar\omega) + [n_{\gamma}(\omega)+1] \\ &\delta(\epsilon-\xi-\hbar\omega)\} + 2\pi \sum_{\gamma'}\sum_{\gamma''} \int d\omega' \int d\omega'' C_{ph-ph}(\omega,\omega',\omega'',\gamma,\gamma',\gamma'') \times \Big\{\frac{1}{2}[n_{\gamma}^{(+)}(\omega) \\ &n_{\gamma'}(\omega')n_{\gamma''}(\omega'') - n_{\gamma}(\omega)n_{\gamma'}^{(+)}(\omega')n_{\gamma''}^{(+)}(\omega'')]\delta(\hbar\omega-\hbar\omega'-\hbar\omega'') + [n_{\gamma}^{(+)}(\omega)n_{\gamma'}^{(+)}(\omega')n_{\gamma'}^{(+)} \\ &(\omega'') - n_{\gamma}(\omega)n_{\gamma'}(\omega')]n_{\gamma''}^{(+)}(\omega'')\delta(\hbar\omega+\hbar\omega'-\hbar\omega'')\Big\} \end{aligned} \tag{2.65}$$

where $n_{\mathbf{Q},\gamma}^{(+)} = 1 + n_{\mathbf{Q},\gamma}$ with γ = LA, TA, and TA2. The expression of coupling functions introduced in Eq.[2.64, 2.65] is given by:

$$C_{e-e}(\epsilon,\epsilon',\xi,\xi') = \frac{1}{\hbar\mathcal{N}(\epsilon)} \sum_{\mathbf{k},\mathbf{k}',\mathbf{q}} |\tilde{V}(\mathbf{q})|^2 \delta(\epsilon-\epsilon_{\mathbf{k}})\delta(\epsilon'-\epsilon_{\mathbf{k}'})\delta(\xi-\epsilon_{\mathbf{k}+\mathbf{q}})\delta(\xi'-\epsilon_{\mathbf{k}'-\mathbf{q}}) \tag{2.66}$$

$$C_{e-ph}(\epsilon,\xi,\omega,\gamma) = \frac{1}{\hbar\mathcal{N}(\epsilon)} \sum_{\mathbf{k},\mathbf{Q}} |\tilde{g}(\mathbf{Q},\gamma)|^2 \delta(\epsilon-\epsilon_{\mathbf{k}})\delta(\xi-\epsilon_{\mathbf{k}+\mathbf{Q}})\delta(\omega-\omega_{\mathbf{Q}\gamma}) \tag{2.67}$$

$$C_{ph-e}(\epsilon,\xi,\omega,\gamma)=\frac{1}{\hbar\mathcal{D}_{\gamma}(\omega)}\sum_{\mathbf{k},\mathbf{Q}}|\tilde{g}(\mathbf{Q},\gamma)|^{2}\delta(\epsilon-\epsilon_{\mathbf{k}})\delta(\xi-\epsilon_{\mathbf{k}+\mathbf{Q}})\delta(\omega-\omega_{\mathbf{Q}\gamma}) \tag{2.68}$$

$$C_{ph-ph}(\omega,\omega',\omega'',\gamma,\gamma',\gamma'')=\frac{1}{\hbar\mathcal{D}_{\gamma}(\omega)}\sum_{\mathbf{Q},\mathbf{Q}'}|\tilde{A}^{\gamma,\gamma',\gamma''}_{\mathbf{Q},\mathbf{Q}',-(\mathbf{Q}+\mathbf{Q}')}|^{2}\delta(\omega-\omega_{\mathbf{Q}\gamma})\delta(\omega'-\omega_{\mathbf{Q}'\gamma'})\delta(\omega''-\omega_{\mathbf{Q}+\mathbf{Q}\gamma''}) \tag{2.69}$$

Eqs.[2.66- 2.69] describes the coupling function for e-e, e-ph, ph-e, and ph-ph scatterings respectively. Now for an isotropic system, above mentioned coupling functions are expressed as:

The e-e coupling function

Eq. 2.66 can be rewritten as

$$\begin{aligned}C_{e-e}(\epsilon,\epsilon';\xi,\xi')=&\frac{1}{4\pi^{2}\epsilon_{f}^{2}}\sqrt{\frac{\epsilon_{f}}{\epsilon}}\frac{\hbar}{ma_{0}^{2}}\int_{0}^{\infty}ds\left[\frac{1}{s^{2}+(q_{TF}/k_{F})^{2}}\right]^{2}\\&\times\theta_{H}[1-h_{1}(\epsilon,\xi,s)]\theta_{H}[1+h_{1}(\epsilon,\xi,s)]\times\theta_{H}[1-h_{1}(\epsilon',\xi',s)]\\&\theta_{H}[1+h_{1}(\epsilon',\xi',s)]\end{aligned} \tag{2.70}$$

where k_F is the Fermi wave number, and the expression of h_1 is given by

$$h_{1}(\epsilon,\xi,s)=\frac{1}{2s}\sqrt{\frac{\epsilon_{F}}{\epsilon}}\left(\frac{\xi}{\epsilon_{F}}-\frac{\epsilon}{\epsilon_{F}}-s^{2}\right) \tag{2.71}$$

The e-ph and ph-e coupling function

$$C_{e-ph}(\epsilon,\xi,\omega,\gamma) = \frac{3Z_{val}}{128}\sqrt{\frac{\epsilon_F}{\epsilon}}\left(\frac{D_\gamma}{\epsilon_F}\right)^2 \frac{(\hbar\omega)^2}{(\frac{1}{2}M_i v_\gamma^2)(\frac{1}{2}m v_\gamma^2)} \times \theta_H[1-h_2(\epsilon,\xi,\omega)]\theta_H[1+h_2(\epsilon,\xi,\omega)] \quad (2.72)$$

where D_γ, M_i, and Z_{val} are the deformation potential, mass of ion, and number of the valence electrons respectively.

$$C_{ph-e}(\epsilon,\xi,\omega,\gamma) = \frac{\mathcal{N}(\epsilon)}{\mathcal{D}_\gamma(\omega)} C_{e-ph}(\epsilon,\xi,\omega,\gamma) \quad (2.73)$$

where $\mathcal{N}(\epsilon)$ is the electron density of states (DOS) per spin and $\mathcal{D}_\gamma(\omega)$ is the phonon density of states (DOS) for the polarization γ. The expression of h_2 is given by

$$h_2(\epsilon,\xi,\omega) = \sqrt{\frac{K_\gamma \epsilon_F^2}{(\hbar\omega)^2\epsilon}}\left[\frac{\xi}{\epsilon_F} - \frac{\epsilon}{\epsilon_F} - \frac{(\hbar\omega)^2}{4K_\gamma\epsilon_F}\right] \quad (2.74)$$

where $K_\gamma = m v_\gamma^2/2$. Also when $\epsilon = \xi = \epsilon_F$ then $C_{e-ph}(\epsilon,\xi,\omega,\gamma)$ is related to the Eliashberg function

$$C_{e-ph}(\epsilon_F,\epsilon_F,\omega,\gamma) = \alpha^2 F(\omega,\gamma)$$

The ph-ph coupling function

$$C_{ph-ph}(\omega,\omega',\omega'',\gamma,\gamma',\gamma'') = \frac{\Omega}{(2\pi)^6\hbar\mathcal{D}_\gamma(\omega)}\left(\frac{\hbar}{2\rho_i}\right)^3 \int dS \int dS' \times \frac{\omega\omega'}{(v_\gamma v_{\gamma'})^3} \frac{|A_{ph}|^2}{v_{\gamma''}|\mathbf{Q}+\mathbf{Q}'|}\delta(\omega'' - v_{\gamma''}|\mathbf{Q}+\mathbf{Q}'|) \quad (2.75)$$

where $\int dS = \int d\theta \sin\theta \int d\phi$. The numerical integrals for above equation are solved by using the efficient spherical designs method[5]. Now using re scaling all the equations in section 2.2, we simplify this model.

2.2.4 Dimensionless equations

We can rewrite the e-e coupling function (see Eq. 2.70) as

$$C_{e-e}(\overline{\epsilon}, \overline{\epsilon}', \overline{\xi}, \overline{\xi}') = \frac{1}{4\pi^2\epsilon_f^2}\frac{\hbar}{ma_0}\sqrt{\frac{1}{\overline{\epsilon}}}\int_{s_{lower}}^{s_{upper}} ds \left(\frac{1}{s^2+\overline{q}^2}\right)^2 \tag{2.76}$$

where $\overline{q} = \frac{q_{TF}}{k_f}$ and $\overline{\epsilon} = \frac{\epsilon}{\epsilon_f}$. Also the integration limits of s can be found out by using the Heaviside step function in Eq. 2.70, and Eq. 2.71 such that

$$\begin{aligned}\frac{1}{2s}\frac{1}{\sqrt{\overline{\epsilon}}}(\overline{\xi} - \overline{\epsilon} - s^2) &\leq 1 \\ \left(s + \sqrt{\overline{\epsilon}}\right)^2 &\geq \overline{\xi} \\ s &\geq \sqrt{\overline{\xi}} - \sqrt{\overline{\epsilon}}\end{aligned}$$

and

$$\begin{aligned}\frac{1}{2s}\frac{1}{\sqrt{\overline{\epsilon}}}(\overline{\xi} - \overline{\epsilon} - s^2) &\geq -1 \\ \left(s - \sqrt{\overline{\epsilon}}\right)^2 &\leq \overline{\xi} \\ s &\leq \sqrt{\overline{\xi}} + \sqrt{\overline{\epsilon}}\end{aligned}$$

Therefore, the bounds of s will be (using Eq. 2.71)

$$\max(\sqrt{\overline{\xi}} - \sqrt{\overline{\epsilon}}, \sqrt{\overline{\xi}'} - \sqrt{\overline{\epsilon}'}) \;\leq\; s \;\leq\; \min(\sqrt{\overline{\xi}} + \sqrt{\overline{\epsilon}}, \sqrt{\overline{\xi}'} + \sqrt{\overline{\epsilon}'})$$

[5]The details of efficient spherical designs with good geometric properties can be obtained from Appendix A.4

The e-ph coupling function (see Eq. 2.72) can be rewritten as

$$\begin{aligned} C_{e-ph}(\overline{\epsilon},\overline{\xi},\overline{\omega},\gamma) &= \frac{3Z_{val}}{32}\frac{\overline{D}_{\gamma}^{2}}{\sqrt{\overline{\epsilon}}}\frac{(\hbar\omega)^2}{K_{\gamma}^{2}}\frac{m}{M_i} \\ &= \frac{3Z_{val}}{32}\frac{\overline{D}_{\gamma}^{2}}{\sqrt{\overline{\epsilon}}}\overline{\omega}^{2}\frac{(\hbar\Omega_{D,LA})^2}{\overline{K}_{\gamma}^{2}\epsilon_f^2}\frac{m}{M_i} \end{aligned} \tag{2.77}$$

where $\Omega_{D,LA}$ is the Debye frequency of LA phonons, $\overline{K}_{\gamma} = K_{\gamma}/\epsilon_F$, $\overline{D}_{\gamma} = D_{\gamma}/\epsilon_F$, and $\overline{\omega} = \omega/\Omega_{D,LA}$. Also he integration limits can be found out by using the Heaviside step function in Eq. 2.74 such that

$$\begin{aligned} \frac{1}{2}\frac{1}{\overline{\omega}}\sqrt{\frac{1}{\overline{\epsilon}}}[\overline{\xi}-\overline{\epsilon}-\overline{\omega}^2] &\leq 1 \\ \overline{\omega}+\sqrt{\overline{\epsilon}} &\geq \sqrt{\overline{\xi}} \\ \overline{\omega} &\geq \sqrt{\overline{\xi}}-\sqrt{\overline{\epsilon}} \end{aligned} \tag{2.78}$$

$$\begin{aligned} \frac{1}{2}\frac{1}{\overline{\omega}}\sqrt{\frac{1}{\overline{\epsilon}}}[\overline{\xi}-\overline{\epsilon}-\overline{\omega}^2] &\geq -1 \\ \overline{\omega}-\sqrt{\overline{\epsilon}} &\geq \sqrt{\overline{\xi}} \\ \overline{\omega} &\leq \sqrt{\overline{\xi}}+\sqrt{\overline{\epsilon}} \end{aligned} \tag{2.79}$$

Therefore, the limits of ω are

$$\omega_D(\sqrt{\overline{\xi}}-\sqrt{\overline{\epsilon}}) \;\leq\; \omega \;\leq\; \omega_D(\sqrt{\overline{\xi}}+\sqrt{\overline{\epsilon}}) \tag{2.80}$$

Similarly, the expression of ph-e coupling function can be written as

$$C_{ph-e}(\overline{\epsilon},\overline{\xi},\overline{\omega},\gamma) = \frac{1}{\hbar}\left(\frac{3\sqrt{2}Z_{val}}{32}\right)\left[\frac{\overline{D}_{\gamma}^{2}}{\sqrt{\overline{K}_{\gamma}}}\left(\frac{m}{M_i}\right)\right] \tag{2.81}$$

For the case of ph-ph coupling function: let us first consider the already defined dimensional ph-ph coupling function

$$C_{ph-ph}(\omega,\omega',\omega'',\gamma,\gamma',\gamma'') = \frac{\Omega}{(2\pi)^6\hbar\mathcal{D}_\gamma(\omega)}\left(\frac{\hbar}{2\rho_i}\right)^3\int dS\int dS'\times\frac{\omega\omega'}{(v_\gamma v_{\gamma'})^3} \\ \frac{|A_{ph}|^2}{v_{\gamma''}|\mathbf{Q}+\mathbf{Q}'|}\delta(\omega''-v_{\gamma''}|\mathbf{Q}+\mathbf{Q}'|)$$

Then the the simplification of above equation is given by[6]:

$$C_{ph-ph}(\omega,\omega',\omega'',\gamma,\gamma',\gamma'') = K_{ph-ph}\,\tilde{C}_{ph-ph}(\overline{\omega},\overline{\omega}',\overline{\omega}'',\gamma,\gamma',\gamma'') \tag{2.82}$$

where K_{ph-ph} is defined as[7]

$$K_{ph-ph} = \left(\frac{1}{4\pi}\right)^4\frac{\hbar}{\Omega_D^2}\frac{B^2}{\rho_i^3}\frac{\Omega_D^6}{v_0^9}$$

and $\tilde{C}_{ph-ph}$ is defined as

$$\tilde{C}_{ph-ph}(\overline{\omega},\overline{\omega}',\overline{\omega}'',\gamma,\gamma',\gamma'') = \frac{1}{(\overline{v}_{\gamma'})^3}\left(\frac{\overline{\omega}'}{\overline{\omega}\,\overline{\omega}''}\right)\theta_H(\Omega_D-\omega)\int dS\int dS'|\overline{A}_{ph}|^2 \\ \delta(\overline{\omega}''-\frac{v_{\gamma''}}{\Omega_D}|\mathbf{Q}+\mathbf{Q}'|)$$

where B $=\rho_i v_0^2$, $\overline{A}_{ph}=\frac{A_{ph}}{BQ_0^3}$, $\overline{v}_\gamma=\frac{v_\gamma}{v_0}$, and $\mathbf{Q}+\mathbf{Q}'=\frac{\overline{\omega}''\Omega_D}{v_{\gamma''}}$. Now after putting all coupling function expressions into the Eqs.[2.64, 2.65], and further solving it, we get

[6]The details can be obtained from Appendix A.5

[7]From now onwards I will denote $\Omega_{D,LA}$ as Ω_D

$$\frac{\partial f(\overline{\epsilon})}{\partial \overline{t}} = \frac{4.556}{\sqrt{\overline{\epsilon}}}\left(\frac{1}{2\overline{q}^3}\right)\int d\overline{\epsilon}'\int d\overline{\xi}\int d\overline{\xi}'\int_{s_{lower}}^{s_{higher}} ds\left(\frac{1}{[s^2+\overline{q}^2]}\right)\delta(\overline{\epsilon}+\overline{\epsilon}'-\overline{\xi}-\overline{\xi}')\left\{-f(\overline{\epsilon})f(\overline{\epsilon}')\right.$$

$$\left.[1-f(\overline{\xi})][1-f(\overline{\xi}')]+[1-f(\overline{\epsilon}][1-f(\overline{\epsilon}']f(\overline{\xi})f(\overline{\xi}')\right\}+\frac{3\pi Z_{val}}{16}\frac{\overline{D_\gamma}^2}{\sqrt{\overline{\epsilon}}}\overline{\omega}^2\frac{(\hbar\Omega_D)^3}{\overline{K}_\gamma^2\epsilon_f^3}\frac{m}{M_i}$$

$$\sum_\gamma\int d\overline{\xi}\int d\overline{\omega}\overline{D}_\gamma^2\overline{\omega}^2\left(\delta\left(\overline{\epsilon}-\overline{\xi}-\frac{\hbar\overline{\omega}\Omega_D}{\epsilon_f}\right)\left\{[f(\overline{\xi})-f(\overline{\epsilon})]n_\gamma(\overline{\omega})-f(\overline{\epsilon})[1-f(\overline{\xi})]\right\}\right.$$

$$\left.+\,\delta\left(\overline{\epsilon}-\overline{\xi}+\frac{\hbar\overline{\omega}\Omega_D}{\epsilon_f}\right)\left\{[f(\overline{\xi})-f(\overline{\epsilon})]n_\gamma(\overline{\omega})+f(\overline{\xi})[1-f(\overline{\epsilon})]\right\}\right) \tag{2.83}$$

where γ can be LA, TA1, TA2. Therefore

$$\frac{\partial f(\overline{\epsilon})}{\partial \overline{t}} = \frac{4.556}{\sqrt{\overline{\epsilon}}}\left(\frac{1}{2\overline{q}^3}\right)\int d\overline{\epsilon}'\int d\overline{\xi}\left(\left[\frac{\overline{q}s}{\overline{q}^2+s^2}+tan^{-1}\left(\frac{s}{\overline{q}}\right)\right]\right)_{s_{lower}}^{s_{upper}}\{-f(\overline{\epsilon})f(\overline{\epsilon}')[1-f(\overline{\xi})]$$

$$[1-f(\overline{\epsilon}+\overline{\epsilon}'-\overline{\xi})]+[1-f(\overline{\epsilon}][1-f(\overline{\epsilon}')]f(\overline{\xi})f(\overline{\epsilon}+\overline{\epsilon}'-\overline{\xi})\}+\frac{3\pi Z_{val}}{16}\frac{\overline{D}_{LA}^2}{\sqrt{\overline{\epsilon}}}\frac{(\hbar\Omega_D)^3}{\overline{K}_{LA}^2\epsilon_f^3}\frac{m}{M_i}\int d\overline{\omega}$$

$$\overline{\omega}^2\left(\left\{\left[f\left(\overline{\epsilon}-\frac{\hbar\overline{\omega}\Omega_D}{\epsilon_f}\right)-f(\overline{\epsilon})\right]n_{LA}(\overline{\omega})-f(\overline{\epsilon})\left[1-f\left(\overline{\epsilon}-\frac{\hbar\overline{\omega}\Omega_D}{\epsilon_f}\right)\right]\right\}+\left\{\left[f\left(\overline{\epsilon}+\frac{\hbar\overline{\omega}\Omega_D}{\epsilon_f}\right)\right.\right.\right.$$

$$\left.\left.\left.-f(\overline{\epsilon})\right]n_{LA}(\overline{\omega})+f\left(\overline{\epsilon}+\frac{\hbar\overline{\omega}\Omega_D}{\epsilon_f}\right)[1-f(\overline{\epsilon})]\right\}\right)+\frac{3\pi Z_{val}}{16}\frac{\overline{D}_{TA1}^2}{\sqrt{\overline{\epsilon}}}\frac{(\hbar\Omega_D)^3}{\overline{K}_{TA1}^2\epsilon_f^3}\frac{m}{M_i}\int d\overline{\omega}\,\overline{\omega}^2$$

$$\left(\left\{\left[f\left(\overline{\epsilon}-\frac{\hbar\overline{\omega}\Omega_D}{\epsilon_f}\right)-f(\overline{\epsilon})\right]n_{TA1}(\overline{\omega})-f(\overline{\epsilon})\left[1-f\left(\overline{\epsilon}-\frac{\hbar\overline{\omega}\Omega_D}{\epsilon_f}\right)\right]\right\}+\left\{\left[f\left(\overline{\epsilon}+\frac{\hbar\overline{\omega}\Omega_D}{\epsilon_f}\right)\right.\right.\right.$$

$$\left.\left.\left.-f(\overline{\epsilon})\right]n_{TA1}(\overline{\omega})+f\left(\overline{\epsilon}+\frac{\hbar\overline{\omega}\Omega_D}{\epsilon_f}\right)[1-f(\overline{\epsilon})]\right\}\right)+\frac{3\pi Z_{val}}{16}\frac{\overline{D}_{TA2}^2}{\sqrt{\overline{\epsilon}}}\frac{(\hbar\Omega_D)^3}{\overline{K}_{TA2}^2\epsilon_f^3}\frac{m}{M_i}\int d\overline{\omega}\,\overline{\omega}^2$$

$$\left(\left\{\left[f\left(\overline{\epsilon}-\frac{\hbar\overline{\omega}\Omega_D}{\epsilon_f}\right)-f(\overline{\epsilon})\right]n_{TA2}(\overline{\omega})-f(\overline{\epsilon})\left[1-f\left(\overline{\epsilon}-\frac{\hbar\overline{\omega}\Omega_D}{\epsilon_f}\right)\right]\right\}+\left\{\left[f\left(\overline{\epsilon}+\frac{\hbar\overline{\omega}\Omega_D}{\epsilon_f}\right)\right.\right.\right.$$

$$\left.\left.\left.-f(\overline{\epsilon})\right]n_{TA2}(\overline{\omega})+f\left(\overline{\epsilon}+\frac{\hbar\overline{\omega}\Omega_D}{\epsilon_f}\right)[1-f(\overline{\epsilon})]\right\}\right) \tag{2.84}$$

where $\bar{t} = t/\tau$ and τ is given by:

$$\tau = \frac{\hbar}{\epsilon_F} = \frac{6.626 \times 10^{-34} J}{2\pi \times 11.695 \times 1.6 \times 10^{-19} J} \quad = 0.0564 \times 10^{-15} seconds \quad = 0.0564\ fs$$

and in our calculation we have used $\bar{t} = 0.01$. Therefore, the time step we have taken is t = 0.564 $\times 10^{-3}$ fs.

$$\frac{\partial n_\gamma(\overline{\omega})}{\partial \bar{t}} = \left(\frac{3\sqrt{2}\pi Z_{val}}{8}\right)\left[\frac{\overline{D_\gamma}^2}{\sqrt{\overline{K_\gamma}}}\left(\frac{m}{M_i}\right)\right]\int d\bar{\epsilon}\int d\bar{\xi}\ f(\bar{\epsilon})[1-f(\bar{\xi})]\left\{-n_\gamma\delta\left(\bar{\epsilon}-\bar{\xi}'+\frac{\hbar\overline{\omega}\Omega_D}{\epsilon_f}\right)\right\}$$

$$[n_\gamma(\overline{\omega})+1]\delta\left(\bar{\epsilon}-\bar{\xi}-\frac{\hbar\overline{\omega}\Omega_D}{\epsilon_f}\right)+\frac{2\pi\Omega_D}{\hbar}\sum_{\gamma'}\sum_{\gamma''}\int d\overline{\omega}'\int d\overline{\omega}'' C_{ph-ph}(\overline{\omega},\overline{\omega}',\overline{\omega}'',\gamma,\gamma',\gamma'')$$

$$\times\left\{\frac{1}{2}[n_\gamma^{(+)}(\overline{\omega})n_{\gamma'}(\overline{\omega}')n_{\gamma''}(\overline{\omega}'')-n_\gamma(\overline{\omega})n_{\gamma'}^{(+)}(\overline{\omega}')n_{\gamma''}^{(+)}(\overline{\omega}'')]\delta\left[(\overline{\omega}-\overline{\omega}'-\overline{\omega}'')\right]\right.$$

$$\left.+[n_\gamma^{(+)}(\overline{\omega})n_{\gamma'}^{(+)}\overline{\omega}'n_{\gamma'}^{(+)}(\overline{\omega}'')-n_\gamma(\overline{\omega})n_{\gamma'}(\overline{\omega}')]n_{\gamma''}^{(+)}(\overline{\omega}'')\delta\left[(\overline{\omega}+\overline{\omega}'-\overline{\omega}'')\right]\right\} \tag{2.85}$$

Again γ can be LA, TA1, TA2, but $\gamma, \gamma', \gamma''$ are restricted by the selection rules I have mentioned earlier in Eqs.[2.33, 2.47, 2.49]. Thus Eq. 2.85 can further be split into three equations correspond to three selection rules.

$$LA(\mathbf{Q}) \rightleftharpoons LA(\mathbf{Q}') + TA1(\mathbf{Q}'')$$

Therefore the time evolution of phonon distribution function for the first selection rule is given by

$$\frac{\partial n_{LA}(\overline{\omega})}{\partial \overline{t}} = \left(\frac{3\sqrt{2}\pi Z_{val}}{8}\right)\left[\frac{\overline{D}_{LA}^2}{\sqrt{\overline{K}_{LA}}}\left(\frac{m}{M_i}\right)\right]\int d\overline{\epsilon}\int d\overline{\xi}\; f(\overline{\epsilon})[1-f(\overline{\xi})]\,\{-n_{LA}(\overline{\omega})$$

$$\delta\left(\overline{\epsilon}-\overline{\xi}'+\frac{\hbar\overline{\omega}\Omega_D}{\epsilon_f}\right)\Big\}\,[n_{LA}(\overline{\omega})+1]\delta\left(\overline{\epsilon}-\overline{\xi}-\frac{\hbar\overline{\omega}\Omega_D}{\epsilon_f}\right)+\frac{2\pi\Omega_D}{\hbar}\sum_{LA}\sum_{TA1}\int d\overline{\omega}'$$

$$\int d\overline{\omega}'' C_{ph-ph}(\overline{\omega},\overline{\omega}',\overline{\omega}'',LA,LA,TA1)\times\Big\{\frac{1}{2}[n_{LA}^{(+)}(\overline{\omega})n_{LA}(\overline{\omega}')n_{TA1}(\overline{\omega}'')-n_{LA}(\overline{\omega})$$

$$n_{LA}^{(+)}(\overline{\omega}')n_{TA1}^{(+)}(\overline{\omega}'')]\delta\left[(\overline{\omega}-\overline{\omega}'-\overline{\omega}'')\right]+[n_{LA}^{(+)}(\overline{\omega})n_{LA}^{(+)}\overline{\omega}'n_{TA1}(\overline{\omega}'')-n_{LA}(\overline{\omega})n_{LA}(\overline{\omega}')]$$

$$n_{TA1}^{(+)}(\overline{\omega}'')\delta\left[(\overline{\omega}+\overline{\omega}'-\overline{\omega}'')\right]\Big\} \tag{2.86}$$

Similarly for the second selection rule:

$$LA(\mathbf{Q})\rightleftharpoons TA1(\mathbf{Q}')+TA1(\mathbf{Q}'')$$

The Eq. 2.85 can be written as:

$$\frac{\partial n_{LA}(\overline{\omega})}{\partial \overline{t}} = \left(\frac{3\sqrt{2}\pi Z_{val}}{8}\right)\left[\frac{\overline{D}_{LA}^2}{\sqrt{\overline{K}_{LA}}}\left(\frac{m}{M_i}\right)\right]\int d\overline{\epsilon}\int d\overline{\xi}\; f(\overline{\epsilon})[1-f(\overline{\xi})]\,\{-n_{LA}(\overline{\omega})$$

$$\delta\left(\overline{\epsilon}-\overline{\xi}'+\frac{\hbar\overline{\omega}\Omega_D}{\epsilon_f}\right)\Big\}\,[n_{LA}(\overline{\omega})+1]\delta\left(\overline{\epsilon}-\overline{\xi}-\frac{\hbar\overline{\omega}\Omega_D}{\epsilon_f}\right)+\frac{2\pi\Omega_D}{\hbar}\sum_{LA}\sum_{TA1}\int d\overline{\omega}'$$

$$\int d\overline{\omega}'' C_{ph-ph}(\overline{\omega},\overline{\omega}',\overline{\omega}'',LA,TA1,TA1)\times\Big\{\frac{1}{2}[n_{LA}^{(+)}(\overline{\omega})n_{TA1}(\overline{\omega}')n_{TA1}(\overline{\omega}'')-n_{LA}(\overline{\omega})$$

$$n_{TA1}^{(+)}(\overline{\omega}')n_{TA1}^{(+)}(\overline{\omega}'')]\delta\left[(\overline{\omega}-\overline{\omega}'-\overline{\omega}'')\right]+[n_{LA}^{(+)}(\overline{\omega})n_{TA1}^{(+)}\overline{\omega}'n_{TA1}(\overline{\omega}'')-n_{LA}(\overline{\omega})n_{TA1}(\overline{\omega}')$$

$$n_{TA1}^{(+)}(\overline{\omega}'')]\delta\left[(\overline{\omega}+\overline{\omega}'-\overline{\omega}'')\right]\Big\} \tag{2.87}$$

Now for the third selection rule:

$$LA(\mathbf{Q}) \rightleftharpoons TA2(\mathbf{Q}') + TA2(\mathbf{Q}'')$$

Then Eq. 2.85 can be written as:

$$\frac{\partial n_{LA}(\overline{\omega})}{\partial \overline{t}} = \left(\frac{3\sqrt{2}\pi Z_{val}}{8}\right)\left[\frac{\overline{D}_{LA}^{2}}{\sqrt{\overline{K}_{LA}}}\left(\frac{m}{M_i}\right)\right]\int d\overline{\epsilon}\int d\overline{\xi}\, f(\overline{\epsilon})[1-f(\overline{\xi})]\,\{-n_{LA}(\overline{\omega})$$

$$\delta\left(\overline{\epsilon}-\overline{\xi}'+\frac{\hbar\overline{\omega}\Omega_D}{\epsilon_f}\right)\Big\}\,[n_{LA}(\overline{\omega})+1]\delta\left(\overline{\epsilon}-\overline{\xi}-\frac{\hbar\overline{\omega}\Omega_D}{\epsilon_f}\right)+\frac{2\pi\Omega_D}{\hbar}\sum_{LA}\sum_{TA2}\int d\overline{\omega}'$$

$$\int d\overline{\omega}'' C_{ph-ph}(\overline{\omega},\overline{\omega}',\overline{\omega}'',LA,TA2,TA2)\times\Big\{\frac{1}{2}[n_{LA}^{(+)}(\overline{\omega})n_{TA2}(\overline{\omega}')n_{TA2}(\overline{\omega}'')-n_{LA}(\overline{\omega})$$

$$n_{TA2}^{(+)}(\overline{\omega}')n_{TA2}^{(+)}(\overline{\omega}'')]\delta\left[(\overline{\omega}-\overline{\omega}'-\overline{\omega}'')\right]+[n_{LA}^{(+)}(\overline{\omega})n_{TA2}^{(+)}\overline{\omega}'n_{TA2}(\overline{\omega}'')-n_{LA}(\overline{\omega})n_{TA2}(\overline{\omega}')$$

$$n_{TA2}^{(+)}(\overline{\omega}'')]\delta\left[(\overline{\omega}+\overline{\omega}'-\overline{\omega}'')\right]\Big\} \tag{2.88}$$

Chapter 3

Results and Discussions

3.1 Introduction

In this chapter we discuss the computational details we need to employ in order to understand the relaxation dynamics of carriers in conventional metals. Followed by computational details we discuss the findings from computational and theoretical (as explained in chapter 2) analysis. We systemically investigate the temporal evolution of electronic and phononic distribution along with the relaxation dynamics of electrons, LA, and TA phonons.

3.2 Computational details

We have studied the thermalization in Aluminum (Al) whose dimensionless Wigner-Seitz radius is $r_s = 2.07$. To analyze the energy relaxation carrier dynamics in metals, we need the numerical values of the elastic constants λ_L, μ_L, E_1, E_2, and E_3. Therefore, to determine the values of the elastic constants of the isotropic system, Ono *et al.* [6] has employed the following procedure:

- First, we define X_2 and X_3 as

$$X_2 = \sum_{ijkl} (G_{ijkl} - Cijkl)^2$$

$$X_3 = \sum_{ijklmn} (G_{ijklmn} - C_{ijklmn})^2 \tag{3.1}$$

  where C_{ijkl}, C_{ijklmn} are the elastic constants of isotropic model and G_{ijkl}, G_{ijklmn} are the elastic constants of a real solid.

- Then the most general definition of G_{ijkl} and G_{ijklmn} may be given by minimizing X_2 and X_3.

Therefore, elastic constants of cubic crystals can be obtained by using this scheme. As a result, the expression for these elastic constants is given by

$$\begin{aligned}
\lambda_L &= \frac{1}{5}(C_{11} + 4C_{12} - 2C_{44}) \\
\mu_L &= \frac{1}{5}(C_{11} - C_{12} + 3C_{44}) \\
E_1 &= \frac{1}{35}C_{111} + \frac{18}{35}C_{112} + \frac{16}{35}C_{123} - \frac{6}{7}C_{144} - \frac{12}{35}C_{155} + \frac{16}{35}C_{456} \\
E_2 &= \frac{1}{35}C_{111} + \frac{4}{35}C_{112} - \frac{1}{7}C_{123} + \frac{19}{35}C_{144} + \frac{2}{35}C_{155} - \frac{12}{35}C_{456} \\
E_3 &= \frac{1}{35}C_{111} - \frac{3}{35}C_{112} + \frac{2}{35}C_{123} - \frac{9}{35}C_{144} + \frac{9}{35}C_{155} + \frac{9}{35}C_{456}
\end{aligned} \tag{3.2}$$

In the Eq. 3.2 mentioned above, Voigt notation is used to simplify the notations in the tensors which is given by

$$11 \to 1,\ 22 \to 2,\ 33 \to 3,\ 12 \to 4,\ 23 \to 5,\ 31 \to 6 \tag{3.3}$$

The C_{ij} and C_{ijk} values in the right hand side of Eq. 3.6 are calculated using Density Functional Theory [7].

The BOE defined in Eqs.[2.88, 2.84] are solved by using Euler method, with a time

Table 3.1: The calculated second-, third-, and fourth-order elastic constants of Aluminum (Al)[7]

C_{11}	110.4	C_{12}	54.5	C_{44}	31.3
C_{111}	-1253	C_{112}	-426	C_{123}	153
C_{144}	-12	C_{166}	-493	C_{456}	-21
C_{1111}	9916	C_{1112}	2656	C_{1122}	3708
C_{1123}	-1000	C_{1144}	-578	C_{1155}	3554
C_{1255}	-91	C_{1266}	4309	C_{1456}	148
C_{4444}	3329	C_{4455}	127		

step of 0.564×10^{-3} fs. The Fermi energy energy for this model is taken as 11.695 eV[6], and the Debye energy for LA phonons in model is given by

$$E_0 = \hbar\Omega_{LA,D} = 65 \ meV$$

200 total discrete energies are considered in the energy range of $\epsilon \in [\epsilon_f - 10E_0, \epsilon_f + 10E_0]$. While for LA phonons 80, and for TA phonons 41 energies are taken.

3.2.1 Initial electron and phonon distribution function

3.2.1.1 Initial electron distribution function

The initial distribution function for electrons is a slight deviation from the thermal-equilibrium distribution function with Gaussian-type peaks above and below the Fermi level, which given as

$$\begin{aligned} f(\epsilon, t=0) &= f_{FD}(\epsilon, T_0) + \sum_{s=\pm} sA_s \exp\left[-\left(\frac{\epsilon - s\epsilon_0}{2W_e}\right)^2\right] \\ &= \frac{1}{\exp\left[\frac{\epsilon-\epsilon_F}{k_B T_0}\right] + 1} + \sum_{s=\pm} sA_s \exp\left[-\left(\frac{\epsilon - s\epsilon_0}{2W_e}\right)^2\right] \end{aligned} \tag{3.4}$$

where $f_{FD}(\epsilon, T_0)$ is the thermal-equilibrium Fermi-Dirac distribution function. ϵ_o, W_e, $A_\pm$ are the peak position, the width, and the peak height. In the calculation we have

done and so to benchmark Shota Ono's results, we have taken $A_{\pm} = 0.1$, $\epsilon_0 = 300$ meV, and $W_e = 50$ meV. Now eq. 3.4 can further be written as:

$$f(\epsilon, t=0) = \frac{1}{\exp[(\overline{\epsilon}-1)/Temp+1]} + \sum_{s=\pm} sA_s \exp\left[-\left(\frac{\overline{\epsilon} - s\overline{\epsilon}_0}{2\overline{W}_e}\right)^2\right] \tag{3.5}$$

where Temp $= k_B T_0/\epsilon_f$, and $\overline{W}_e = W_e/\epsilon_f$. The effective electron temperature is taken as 800 K.

3.2.1.2 Initial LA phonon distribution function

Since due to electron-photon interaction, electron distribution changes as defined in Eq. 3.4, but during finite-pulse width phonons are also created due to ph-e scatterings, which will disturb the phonon distribution as well, and the initial phonon distribution function is given by

$$\begin{aligned} n_{LA}(\omega, t=0) &= n_{BE}(\omega, T_0) + B\exp\left[-\left(\frac{\omega - \Omega_{LA,D}}{2W_{ph}/\hbar}\right)^2\right] \\ &= \frac{1}{\exp\left[\frac{\hbar\omega}{k_B T_0}\right] - 1} + B\exp\left[-\left(\frac{\omega - \Omega_{LA,D}}{2W_{ph}/\hbar}\right)^2\right] \end{aligned} \tag{3.6}$$

where $n_{BE}(\omega, T_0)$ is the thermal-equilibrium Bose-Einstein distribution function. W_{ph}, B are the peak width, and the peak height. In our calculations we have and to benchmark Shota Ono's results, we have taken $A = 0.01$, and $W_{ph} = 20$ meV. Now eq. 3.6 can further be written as:

$$n_{LA}(\overline{\omega}, t=0) = \frac{1}{\exp\left[\frac{\overline{\omega}\times\hbar\Omega_{LA,D}}{k_B T_0}\right] - 1} + B\exp\left[-\left(\frac{(\overline{\omega}-1)\hbar\Omega_{LA,D}}{2W_{ph}}\right)^2\right] \tag{3.7}$$

where $\overline{\omega} = \omega/\Omega_D$, and $T_0 = 300$ K

3.2.1.3 Initial TA phonon distribution function

Initial distribution function for TA phonons is same as thermal-equilibrium Bose-Einstein phonon distribution function, which is given by

$$n_{TA}(\omega, t=0) = \frac{1}{\exp\left[\frac{\hbar\omega}{k_B T_0}\right] - 1}$$

$$n_{TA}(\overline{\omega}, t=0) = \frac{1}{\exp\left[\frac{\overline{\omega}\times\hbar\Omega_D}{k_B T_0}\right] - 1} \tag{3.8}$$

where $\overline{\omega} = \omega/\Omega_D$, $T_0 = 300$ K, and Ω_D is Debye frequency of LA phonons.

3.3 Results and Conclusions

The electron and LA phonon distribution function is plotted at time t = 10 fs for various time steps in Fig. 3.1 and Fig. 3.2 by using the Euler method.

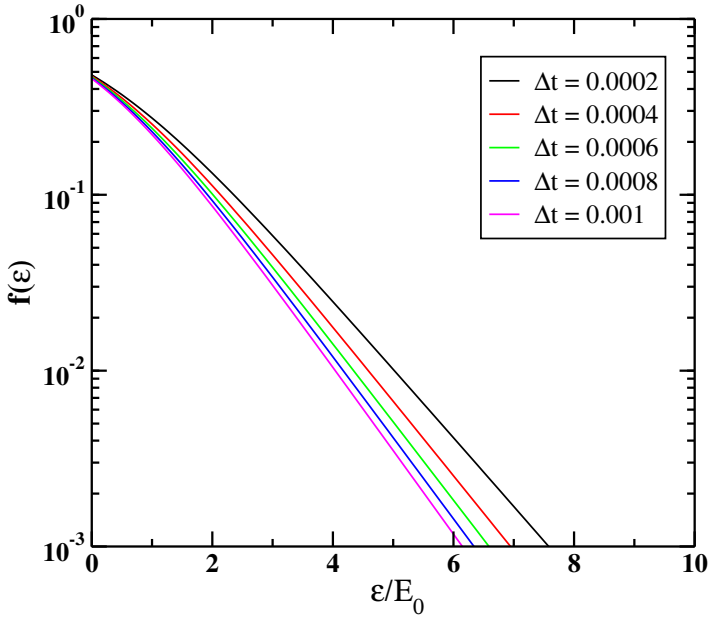

Figure 3.1: The electron distribution function is plotted at t = 10 fs for various time steps Δt

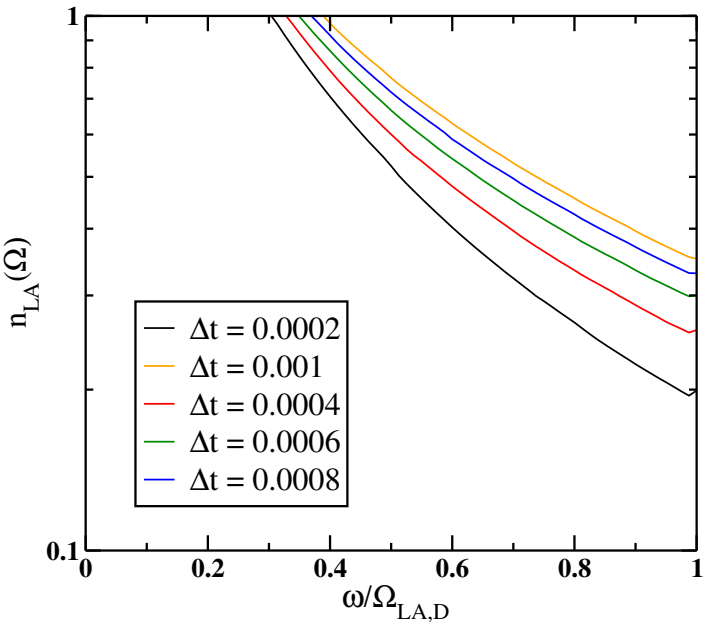

Figure 3.2: The LA phonon distribution function is plotted at t = 10 fs for various time steps Δt

The initial temperature of electrons, and phonons is kept at 800 K, and 300 K. Therefore, we can see from the above mentioned figures that as we decrease the time step value (from $\Delta t = 0.001$ to $\Delta t = 0.0002$), we get a very small change in both electrons and phonons distribution function as compared to higher time step value (Δt), which is more accurate. Thus, Euler method is very sensitive with respect to time step value. But with extremely small time step we can not achieve complete relaxation of phonons and electrons using our current computational facilities.

Therefore, we need more accurate algorithms with small time step values e.g. second-order Runge-Kutta (RK2) method, RK4 method, RK6 method, etc. In our analysis, we employ RK2 method (see Fig. 3.3) with time step $\Delta t = 0.01$, and we have found that with the small time steps variation there is no change or negligible change in phonon distribution function at time t = 10 fs. So we have tried to benchmark the results obtained by Shota Ono (see [6]) using RK2, though the author used RK4 method to track the relaxation dynamics of carriers in [6]. Now since RK4 is more accurate and efficient than RK2, we expect a slight change in the results obtained by us.

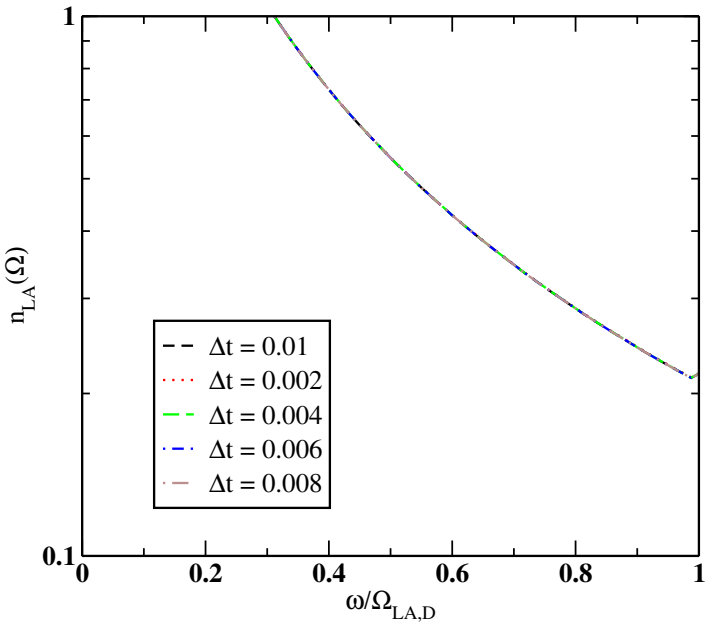

Figure 3.3: The LA phonon distribution function is plotted at t = 10 fs for various time steps Δt using RK2 method

The electronic f (ϵ) and phononic $n_{LA}(\omega)$ distribution function temporal evolution is plotted by Eqs.[2.84, 2.86, 2.87, 2.88] using the above mentioned computational details

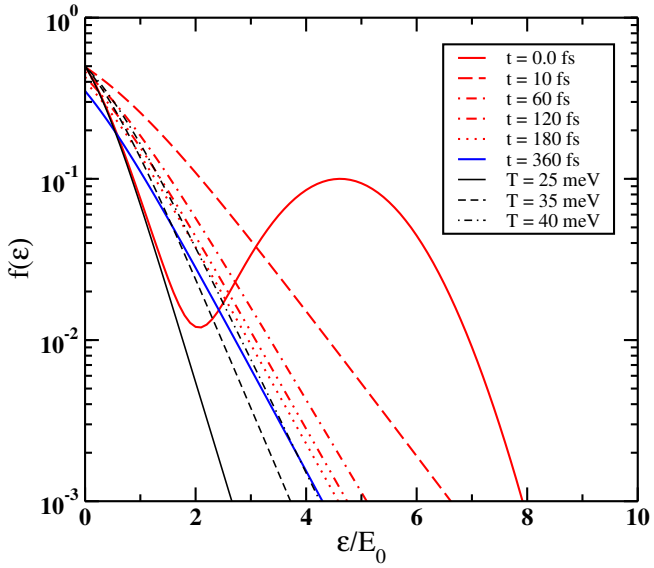

Figure 3.4: The f(ϵ) for various ts and Fermi-Dirac (FD) distribution with several temperatures is plotted.

(see Fig. 3.4 and Fig. 3.6). In both the Fig.[3.4, 3.6], the Fermi-Dirac distribution functions (FD) and Bose-Einstein distribution functions (BE) with several Ts are also shown for the comparison. Therefore, in Fig. 3.4, we compare and benchmark the results obtained by us with the results obtained by Shota Ono (see Fig. 3.5). At t = 360 fs, nonequilibrium electron distribution function is almost coinciding with the Fermi-Dirac distribution curve at Temperature T = 464 K (40 meV). Therefore, we can say that after t = 0.36 ps, the electron distribution can be treated as quasiequilibrium distribution function. However, upto t $\sim$ 0.12 ps, LA phonon population increases due to the presence of ph-e scattering. The phonon population increases with time and is maximum at t = 0.12 ps. After t $\sim$ 0.12 ps the phonon population starts decreasing, as we can can observe the phonon distribution function curve at t = 0.36 ps (solid blue line curve) in Fig. 3.6. The similar behaviour is reported in [6] (see Fig. 3.7).
In our calculations, the initially present Gaussian peak which was observed at $\epsilon/E_0 =$ 5 in f (ϵ) is smeared out very quickly within 10 fs.

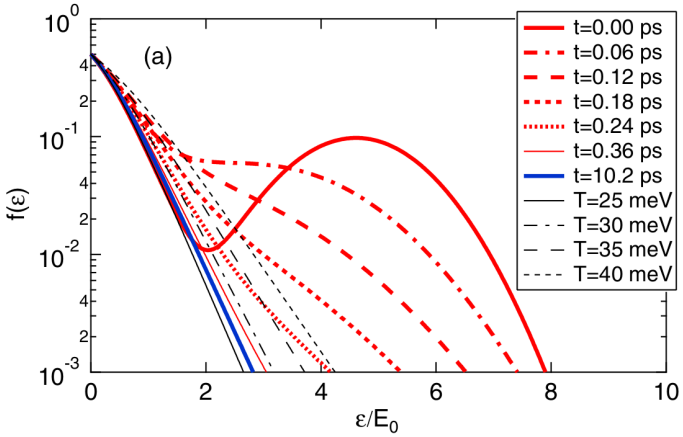

Figure 3.5: This figure represent the f (ϵ) for various ts and FD distribution with several Ts. This figure is taken from [6]

However, the same dynamics is slower in Fig. 3.5. There might be many reasons for this different behaviour e.g.

- In our calculations, the phonon-phonon coupling is not making a significant change in the distribution function.

- There might be some flaw in our coded program. As a result, we are still debugging the code by revisiting all the coefficients used and other errors.

- In [6], the author has used RK4 method. While we are using RK2 method which gives less accurate results compared to RK4 method.

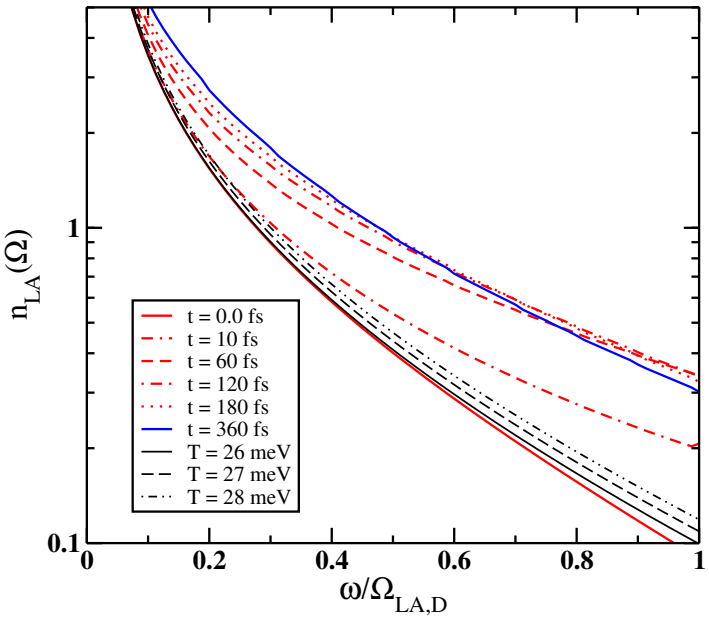

Figure 3.6: The $n_{LA}(\omega)$ for various ts and the Bose-Einstein (BE) distribution with several temperatures is plotted.

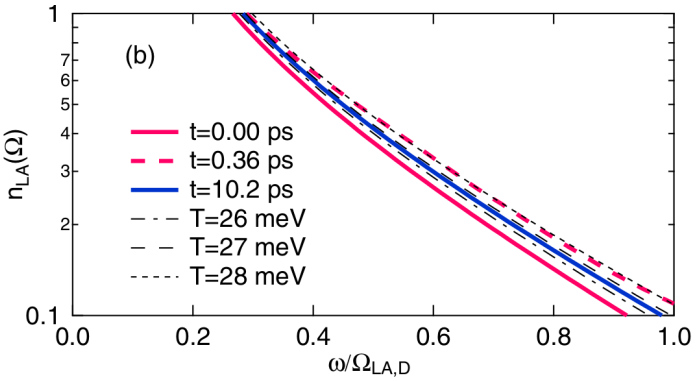

Figure 3.7: The image shows the $n_{LA}(\omega)$ for various ts and the BE distribution with several Ts. This figure is taken from [6]

- The author in [6] has taken 1600 electron energies in the energy window of $\epsilon \in [\epsilon_f - 10E_0, \epsilon_f + 10E_0]$. But till now we could do computation only for 200 energies and upto t = 360 fs.

We have also investigated the electron relaxation dynamics in the presence and absence of electron-phonon coupling. In Fig. 3.8, we have studied the out-of-equilibrium electronic distribution function in the absence of e-ph coupling for various times and then the distributions are compared with Fermi-Dirac distribution (FD) function at temperature T = 800 K.

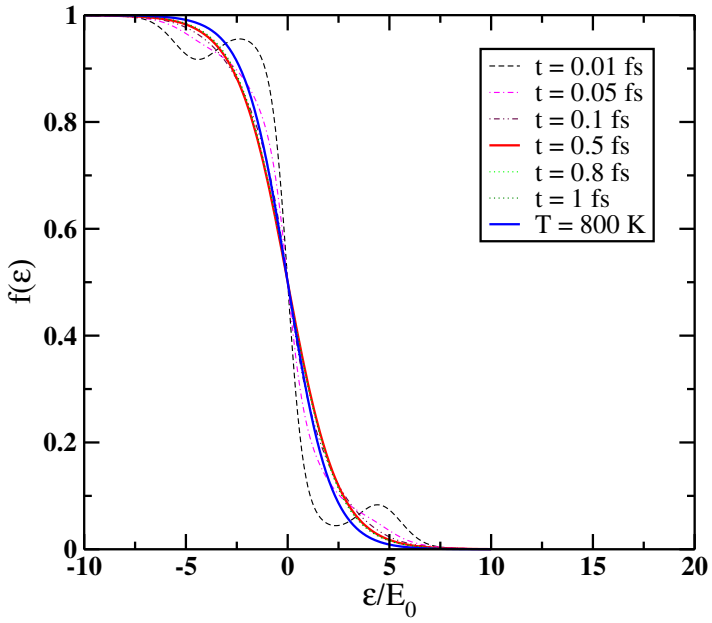

Figure 3.8: The electron distribution functions is plotted for several ts in the absence of electron-phonon coupling and compared with the Fermi-Dirac distribution function (FD) at T = 800 K

We have found that electrons equilibrate at time t$\sim$ 0.5 fs (see solid red line curve), and leaves the electrons subsystem at an effective temperature T $\sim$ 800 K. Therefore after time t $\sim$ 1 fs, electrons can be treated using quasi-thermal equilibrium model provided the phonon don't play any role in the electrons relaxation process or when e-ph coupling is zero.

We have also investigated the electron and phonon relaxation dynamics in the pres-

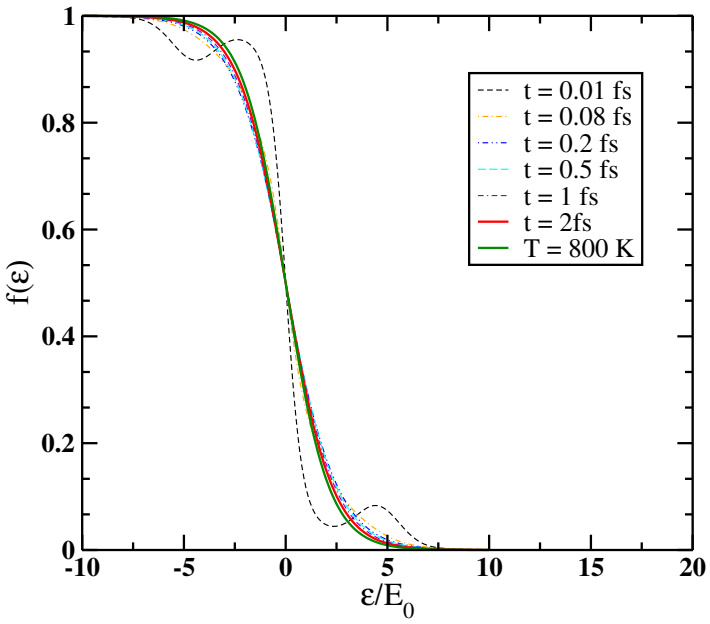

Figure 3.9: The electron distribution functions is plotted for several ts in the presence of electron-phonon coupling and compared with the Fermi-Dirac distribution function (FD) at T = 800 K

ence of e-ph coupling (see Fig. 3.9, 3.10). From Fig. 3.9, we see that in the presence of e-ph coupling, the electrons equilibrate at t $\sim$ 2 fs which is slower compared to the previous case when e-ph coupling was not present. The reason for that might be the

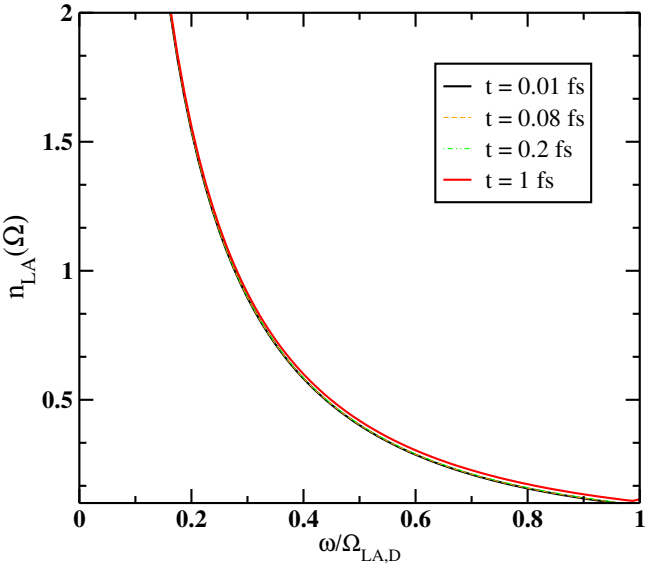

Figure 3.10: The LA phonon distribution functions is plotted for several ts in the presence of e-ph and ph-e coupling.

backward energy flow from phonons to electrons via ph-e coupling. While there is a huge change in the electron distribution function as well as in the electrons temperature at t $\sim$ 1 fs, the change in the LA phonon distribution function is very small and thus the TA phonons will still be cold at t $\sim$ 1 fs, and T = 300 K (see Fig. 3.10). So, we have found that in the initial stage of relaxation, most of the electron energy is transferred into the LA phonons through e-ph, and ph-e scattering. Therefore after t $\sim$ 2 fs, the electrons distribution can be described by using some effective temperature model. Since after 2 fs instead of electrons distribution, temperature is evolving with time and thus to describe the electron distribution time evolution, we don't need full nonequilibrium lattice model.

3.4 Future Work

We have done the relaxation dynamics analysis of the laser excited carriers by solving Boltzmann transport equations taking into account the relevant scattering mechanisms. We have found that the relaxation time for phonons (t>0.36 ps) is much higher than electrons. However till now we have reached upto 0.36 ps. Also we have found some mismatches from the reported results [6]. Therefore, our first future goal is to include the phonon-phonon coupling part into our analysis and then benchmark the results reported in [6]. Since to study the relaxation dynamics of phonons, we need to go upto 10.2 ps, and thus our next goal will be to parallel the code and study the phonons dynamics.

Appendix A

A.1 Calculation of TA phonon frequencies

Details of the relation between various elastic constants and Lam$\acute{e}$ constants as defined already on Page 22,

$$\text{For i} = 1, \quad \rho_i \omega_\gamma^2(\mathbf{Q}) e_1(\mathbf{Q},\gamma) = ((\lambda_L + 2\mu_L)Q_1^2 + \mu_L Q_2^2 + \mu_L Q_3^2) e_1(\mathbf{Q},\gamma) \tag{A.1}$$

$$\text{For i} = 2, \quad \rho_i \omega_\gamma^2(\mathbf{Q}) e_2(\mathbf{Q},\gamma) = (\mu_L Q_1^2 + (\lambda_L + 2\mu_L)Q_2^2 + \mu_L Q_3^2 e_2)(\mathbf{Q},\gamma) \tag{A.2}$$

$$\text{For i} = 3, \quad \rho_i \omega_\gamma^2(\mathbf{Q}) e_3(\mathbf{Q},\gamma) = (\mu_L Q_1^2 + \mu_L Q_3^2 + (\lambda_L + 2\mu_L)Q_3^2 e_3)(\mathbf{Q},\gamma) \tag{A.3}$$

for γ=TA1 and TA2, the wave vector is in perpendicular direction of component of polarization. Hence Eq.[A.1- A.3], will further reduced to

$$\rho_i \omega_\gamma^2(\mathbf{Q}) e_1(\mathbf{Q},\gamma) = (\mu_L Q_2^2 + \mu_L Q_3^2) e_1(\mathbf{Q},\gamma)$$
$$\rho_i \omega_\gamma^2(\mathbf{Q}) e_2(\mathbf{Q},\gamma) = (\mu_L Q_1^2 + \mu_L Q_3^2) e_2(\mathbf{Q},\gamma)$$
$$\rho_i \omega_\gamma^2(\mathbf{Q}) e_3(\mathbf{Q},\gamma) = (\mu_L Q_1^2 + \mu_L Q_2^2) e_3(\mathbf{Q},\gamma)$$

After adding the above mentioned equations, we get

$$\rho_i \omega_\gamma^2(\mathbf{Q}) = 2\mu_L(Q_1^2 + Q_2^2 + Q_3^2)$$
$$\rho_i \omega_\gamma^2(\mathbf{Q}) = 2\mu_L|\mathbf{Q}|^2 \tag{A.4}$$

The above Eq. A.4 has components for both TA1, and TA2. Therefore we can rewrite Eq. A.4 as

$$\rho_i \left(\omega_{TA1}^2(\mathbf{Q}) + \omega_{TA2}^2(\mathbf{Q})\right) = 2\mu_L|\mathbf{Q}|^2 \tag{A.5}$$

Hence Eq. A.5 is valid when $\omega_{TA1} = \omega_{TA2}$. Therefore

$$\rho_i \omega_{TA1}^2(\mathbf{Q}) = \mu_L|\mathbf{Q}|^2$$
$$\omega_{TA1}(\mathbf{Q}) = \sqrt{\frac{\mu_L}{\rho_i}}|\mathbf{Q}|$$

Similarly

$$\rho_i \omega_{TA2}^2(\mathbf{Q}) = \mu_L|\mathbf{Q}|^2$$
$$\omega_{TA2}(\mathbf{Q}) = \sqrt{\frac{\mu_L}{\rho_i}}|\mathbf{Q}|$$

$\Longrightarrow$

$$\omega_{TA1}(\mathbf{Q}) = \omega_{TA2}(\mathbf{Q}) = \sqrt{\frac{\mu_L}{\rho_i}}|\mathbf{Q}| = v_{TA}|\mathbf{Q}| \tag{A.6}$$

where v_{TA} is the TA phonon velocity.

A.2 Representation of the phonon wave vector and the polarization vectors

We can express the phonon wave vector and the polarization vectors using the spherical coordinates. Their representation is given as:

$$\begin{aligned}
\mathbf{Q} &= Q\mathbf{e}_r \\
\mathbf{e}(\mathbf{Q}, LA) &= \mathbf{e}_r = (\sin\theta\cos\phi, \sin\theta\sin\phi, \cos\theta) \\
\mathbf{e}(\mathbf{Q}, TA1) &= \mathbf{e}_\theta = (\cos\theta\cos\phi, \cos\theta\sin\phi, -\sin\theta) \\
\mathbf{e}(\mathbf{Q}, TA2) &= \mathbf{e}_\phi = (-\sin\phi, \cos\phi, 0)
\end{aligned} \tag{A.7}$$

where we employ abbreviated notations $\theta = \theta_{\mathbf{Q}}$ and $\phi = \phi_{\mathbf{Q}}$ etc. Similarly,

$$\begin{aligned}
\mathbf{Q}' &= Q'\mathbf{e}_{r'} \\
\mathbf{e}(\mathbf{Q}', LA) &= \mathbf{e}_{r'} = (\sin\theta'\cos\phi', \sin\theta'\sin\phi', \cos\theta') \\
\mathbf{e}(\mathbf{Q}', TA1) &= \mathbf{e}_{\theta'} = (\cos\theta'\cos\phi', \cos\theta'\sin\phi', -\sin\theta') \\
\mathbf{e}(\mathbf{Q}', TA2) &= \mathbf{e}_{\phi'} = (-\sin\phi', \cos\phi', 0)
\end{aligned} \tag{A.8}$$

where the abbreviation of $\theta' = \theta_{\mathbf{Q}'}$ and $\phi' = \phi_{\mathbf{Q}'}$ is used.

A.3 Details of the allowed scattering processes

The first selection rule

$$LA(\mathbf{Q}) \rightleftharpoons LA(\mathbf{Q}') + TA1(\mathbf{Q}'') \tag{A.9}$$

is discussed already, and the solution for this process is also derived in Eq. 2.46. Now let us consider the second allowed scattering process

$$LA(\mathbf{Q}) \rightleftharpoons TA1(\mathbf{Q}') + TA1(\mathbf{Q}'')$$

where $\mathbf{Q}'' = (\mathbf{Q} - \mathbf{Q}')$, and let $\mathbf{Q} = Q\hat{k}$, Therefore

$$\begin{aligned} \mathbf{Q}''.\hat{k} = Q''.\cos\theta'' &= (\mathbf{Q} - \mathbf{Q}').\hat{k} \\ \implies \cos\theta'' &= \frac{Q - Q'\cos\theta'}{Q''} \end{aligned} \tag{A.10}$$

Similarly

$$\begin{aligned} \mathbf{Q}''.\hat{i} = Q''.\sin\theta''\cos\phi'' &= (\mathbf{Q} - \mathbf{Q}').\hat{i} \\ \implies \sin\theta'' &= -Q'\frac{\sin\theta'\cos\phi'}{Q''\cos\phi''} \end{aligned} \tag{A.11}$$

and

$$\begin{aligned} \mathbf{Q}''.\hat{j} = Q''.\sin\theta''\sin\phi'' &= (\mathbf{Q} - \mathbf{Q}').\hat{j} \\ \implies \sin\theta'' &= -Q'\frac{\sin\theta'\sin\phi'}{Q''\sin\phi''} \end{aligned} \tag{A.12}$$

Now after comparing Eq. A.11 and Eq. A.12, we get

$$\phi' = \phi''$$

Therefore

$$\sin\theta'' = \left(\frac{-Q'}{Q''}\right)\sin\theta'$$

Since this scattering process also involves TA phonons, therefore the **First** term doesn't contribute to Eq. 2.32. Now let us take the **second** term in Eq. 2.32

$$\begin{aligned}
\mathbf{e}.\mathbf{Q} &= Q \\
\mathbf{e}'.\mathbf{e}'' &= \frac{Q\cos\theta' - Q'}{Q''} \\
\mathbf{Q}'.\mathbf{Q}'' &= Q'(Q\cos\theta' - Q') \\
\mathbf{e}'.\mathbf{Q}'' &= -Q\sin\theta' \\
\mathbf{e}''.\mathbf{Q}' &= \frac{QQ'}{Q''}\sin\theta'
\end{aligned}$$

Therefore the second term of Eq. 2.32 is

$$E_2\frac{QQ'}{Q''}[(Q\cos\theta' - Q')^2 - Q^2\sin^2\theta'] \tag{A.13}$$

For both **third** and **forth** terms in Eq. 2.32, because of the presence of two TA1 phonon modes,

$$\mathbf{e}'.\mathbf{Q}' = \mathbf{e}''.\mathbf{Q}'' = 0$$

Now for the **fifth** term,

$$\begin{aligned}
\mathbf{e}.\mathbf{e}' &= -\sin\theta' \\
\mathbf{e}''.\mathbf{Q} &= \frac{QQ'}{Q''}\sin\theta' \\
\mathbf{Q}.\mathbf{Q}'' &= Q(Q - Q'\cos\theta')
\end{aligned}$$

Therefore the fifth term of Eq. 2.32 is

$$E_3 \left(\frac{QQ'}{Q''} \right) \sin^2 \theta' [Q'^2 - Q^2] \tag{A.14}$$

Now for the **sixth** term,

$$\mathbf{e}.\mathbf{Q}' = Q' \cos \theta'$$

Therefore the sixth term of Eq. 2.32 is

$$2E_3 \frac{QQ'}{Q''} Q' \cos \theta' (Q \cos \theta' - Q') \tag{A.15}$$

Now for the **seventh** term,

$$\mathbf{e}.\mathbf{e}'' = \frac{Q'}{Q''} \sin \theta'$$

$$\mathbf{e}'.\mathbf{Q} = -Q \sin \theta'$$

$$\mathbf{Q}.\mathbf{Q}' = QQ' \cos \theta'$$

Therefore the seventh term of Eq. 2.32 is

$$E_3 \frac{QQ'}{Q''} [-Q'(Q \cos \theta' - Q') \sin^2 \theta' - QQ' \sin^2 \theta' \cos \theta'] \tag{A.16}$$

Now for the **eighth** term,

$$\mathbf{e}.\mathbf{Q}'' = Q - Q' \cos \theta'$$

Therefore the eighth term of Eq. 2.32 is

$$E_3 \frac{QQ'}{Q''} [(Q - Q' \cos \theta')(Q \cos \theta' - Q') \cos \theta' - Q \sin^2 \theta' (Q - Q' \cos \theta')] \tag{A.17}$$

Using the above solve expressions, we can see that the the solution of the **ninth** term in Eq. 2.32 is

$$\lambda_L \frac{QQ'}{Q''}(Q\cos\theta' - Q')^2 \tag{A.18}$$

Also the **Tenth** term of Eq. 2.32 is given by

$$2\mu_L((Q' - Q\cos\theta')^2 - Q^2\sin^2\theta') \tag{A.19}$$

The A_{ph} solution for Eq. A.9 is given by:

$$A_{ph} = \frac{QQ'}{Q''}[E_2 + \lambda_L + 2(E_3 + \mu_L)](Q' - Q\cos\theta)^2 - (E_2 + 2E_3 + \mu_L)Q^2\sin^2\theta' \tag{A.20}$$

Now let us consider the third allowed scattering process

$$LA(\mathbf{Q}) \rightleftharpoons TA2(\mathbf{Q}') + TA2(\mathbf{Q}'') \tag{A.21}$$

After doing the similar procedure from Eq. A.10 to Eq. A.12, we get:

$$\mathbf{Q}''.\hat{k} = Q''.\cos\theta'' = (\mathbf{Q} - \mathbf{Q}').\hat{k}$$
$$\implies \cos\theta'' = \frac{Q - Q'\cos\theta'}{Q''}$$

and

$$\sin\theta'' = \left(\frac{-Q'}{Q''}\right)\sin\theta'$$

Again due to the presence of the TA phonons, the first term of the Eq. 2.32 will not contribute to the calculation of A_{ph}. Therefore for the **second** term

$$\mathbf{e}.\mathbf{Q} = Q$$
$$\mathbf{e}'.\mathbf{e}'' = 1$$
$$\mathbf{Q}'.\mathbf{Q}'' = Q'(Q\cos\theta' - Q')$$

$$\mathbf{e}'.\mathbf{Q}'' = 0$$

Therefore the second term of Eq. 2.32 is

$$E_2[QQ'(Q\cos\theta' - Q')] \tag{A.22}$$

Again for both **third** and **forth** terms in Eq. 2.32, because of the presence of two TA2 phonon modes,

$$\mathbf{e}'.\mathbf{Q}' = \mathbf{e}''.\mathbf{Q}'' = 0$$

and **fifth** term will also be zero because

$$\mathbf{e}.\mathbf{e}' = 0$$

Now for the **sixth** term

$$\begin{aligned}\mathbf{e}.\mathbf{Q}' &= Q'\cos\theta' \\ \mathbf{e}''.\mathbf{Q} &= 0 \\ \mathbf{Q}.\mathbf{Q}'' &= Q(Q - Q'\cos\theta')\end{aligned}$$

Therefore the sixth term of Eq. 2.32 is

$$E_3[QQ'\cos\theta'(Q - Q'\cos\theta')] \tag{A.23}$$

The **seventh** term in Eq. 2.32 is 0 because

$$\mathbf{e}.\mathbf{e}'' = 0 \tag{A.24}$$

Now for the **eighth** term:

$$\mathbf{e}.\mathbf{Q}'' = Q - Q'\cos\theta'$$
$$\mathbf{e}'.\mathbf{Q} = 0$$
$$\mathbf{Q}.\mathbf{Q}' = QQ'\cos\theta'$$

Therefore the eighth term of Eq. 2.32 is

$$E_3[QQ'\cos\theta'(Q - Q'\cos\theta')] \tag{A.25}$$

Using the above solve expressions, we can see that the the solution of the **ninth** term in Eq. 2.32 is

$$\lambda_L[QQ'(Q\cos\theta' - Q')] \tag{A.26}$$

Also the **Tenth** term of Eq. 2.32 is given by

$$2\mu_L[QQ'\cos\theta'(Q - Q'\cos\theta')] \tag{A.27}$$

The A_{ph} solution for Eq. A.3 is given by:

$$A_{ph} = QQ'[(E_2 + \lambda_L)(Q\cos\theta' - Q') + 2(E_3 + \mu_L)(Q - Q'\cos\theta')\cos\theta'] \tag{A.28}$$

A.4 Efficient spherical designs method

Efficient spherical designs method helps us to evaluate the numerical integrals for θ and ϕ. Efficient spherical designs are sets of N points x_j, j = 1,...,N on unit sphere S^2 such that these points on the sphere will have equal weights. The files of points set for degrees t = 1, 2, 3, ...180 can be found here[31]. There are some points that should be noted:

- For each point set, the text file has three items per row: the x_j, y_j, and z_j Cartesian coordinates in [-1, 1] for the point $\mathbf{x}_j = (x_j, y_j, z_j)$ on S^2.
- The equal cubature weight for j = 1, 2, 3, 4, ..., N is given by

$$w_j = \frac{|S|^2}{N}$$

- The area of Unit sphere S^2 is given by $|S^2| = 4\pi$
- These spherical t - designs on S^2 have points

$$N = \frac{t^2}{2} + t + O(1)$$

- All points are on the unit sphere such that $|\mathbf{x}_j|^2 = x_j^2 + y_j^2 + z_j^2 = 1$ for all j = 1, 2, 3, ..., N.

A.5 Details of phonon-phonon coupling function

Let us first consider the phonon-phonon (ph-ph) coupling function,

$$C_{ph-ph}(\omega,\omega',\omega'',\gamma,\gamma',\gamma'') = \frac{\Omega}{(2\pi)^6\hbar\mathcal{D}_\gamma(\omega)}\left(\frac{\hbar}{2\rho_i}\right)^3\int dS\int dS'\times\frac{\omega\omega'}{(v_\gamma v_{\gamma'})^3}$$
$$\frac{|A_{ph}|^2}{v_{\gamma''}|\mathbf{Q}+\mathbf{Q}'|}\delta(\omega''-v_{\gamma''}|\mathbf{Q}+\mathbf{Q}'|) \tag{A.29}$$

where $\mathcal{D}_\gamma(\omega)$ is given by

$$\mathcal{D}_\gamma(\omega) = \frac{\Omega\omega^2}{(2\pi^2 v_\gamma^3)}\theta_H(\Omega_{\gamma,D}-\omega)$$

Therefore after putting the $\mathcal{D}_\gamma(\omega)$ expression into Eq. A.29, we get

$$C_{ph-ph}(\omega,\omega',\omega'',\gamma,\gamma',\gamma'') = \frac{\hbar^2}{(4\pi)^4\omega\rho_i^3}\theta_H(\Omega_D-\omega)\int dS\int dS'\times\frac{\omega'}{v_{\gamma''}v_{\gamma'}^3}$$
$$\frac{|A_{ph}|^2}{|\mathbf{Q}+\mathbf{Q}'|}\delta(\omega''-v_{\gamma''}|\mathbf{Q}+\mathbf{Q}'|) \tag{A.30}$$

$$C_{ph-ph}(\overline{\omega},\overline{\omega}',\overline{\omega}'',\gamma,\gamma',\gamma'') = \frac{\hbar^2}{(4\pi)^4\Omega_D\ \rho_i^3}\frac{1}{(v_{\gamma'})^3}\left(\frac{\overline{\omega}'}{\overline{\omega}}\right)\theta_H(\Omega_D-\omega)\int dS\int dS'$$
$$\frac{|A_{ph}|^2}{\overline{\omega}''\Omega_D}\ \frac{v_{\gamma''}}{v_{\gamma'}}\ \delta(\overline{\omega}''-\frac{v_{\gamma''}|\mathbf{Q}+\mathbf{Q}'|}{\Omega_D}) \tag{A.31}$$

from delta function in the right-hand-side:

$$|\mathbf{Q}+\mathbf{Q}'| = \frac{\overline{\omega}''\ \Omega_D}{v_{\gamma''}}$$

where $\overline{\omega}'' = \omega/\Omega_D$. Now Eq. A.31 can be modified as

$$C_{ph-ph}(\overline{\omega},\overline{\omega}',\overline{\omega}'',\gamma,\gamma',\gamma'') = \frac{\hbar^2}{(4\pi)^4\Omega_D^2}\frac{B^2Q_0^6}{(v_{\gamma'})^3\rho_i^3}\left(\frac{\overline{\omega}'}{\overline{\omega}\ \overline{\omega}''}\right)\theta_H(\Omega_D-\omega)\int dS\int dS' \left(\frac{|A_{ph}|}{BQ_0^3}\right)^2\delta(\overline{\omega}'' - \frac{v_{\gamma''}|\mathbf{Q}+\mathbf{Q}'|}{\Omega_D}) \tag{A.32}$$

where $B = \rho_i\, v_0^2$ and $\mathbf{Q}_0 = \Omega_D/v_0$. So, Eq. A.32 can be written as:

$$C_{ph-ph}(\omega,\omega',\omega'',\gamma,\gamma',\gamma'') = K_{ph-ph}\,\tilde{C}_{ph-ph}(\overline{\omega},\overline{\omega}',\overline{\omega}'',\gamma,\gamma',\gamma'') \tag{A.33}$$

where K_{ph-ph} is defined as

$$K_{ph-ph} = \left(\frac{1}{4\pi}\right)^4\frac{\hbar}{\Omega_D^2}\frac{B^2}{\rho_i^3}\frac{\Omega_D^6}{v_0^9}$$

and $\tilde{C}_{ph-ph}$ is defined as

$$\tilde{C}_{ph-ph}(\overline{\omega},\overline{\omega}',\overline{\omega}'',\gamma,\gamma',\gamma'') = \frac{1}{(\overline{v}_{\gamma'})^3}\left(\frac{\overline{\omega}'}{\overline{\omega}\,\overline{\omega}''}\right)\theta_H(\Omega_D-\omega)\int dS\int dS'|\overline{A}_{ph}|^2 \delta(\overline{\omega}'' - \frac{v_{\gamma''}}{\Omega_D}|\mathbf{Q}+\mathbf{Q}'|) \tag{A.34}$$

where the expression of $|\overline{A}_{ph}|$ is defined as

$$|\overline{A}_{ph}| \quad = \quad \frac{A_{ph}}{BQ_0^3}$$

and the numerical integrals for θ, and ϕ are evaluated using spherical designs method.

Bibliography

[1] Bradley Ferguson and Xi-Cheng Zhang. Materials for terahertz science and technology. *Nature materials*, 1(1):26–33, 2002.

[2] Margherita Maiuri, Marco Garavelli, and Giulio Cerullo. Ultrafast spectroscopy: state of the art and open challenges. *Journal of the American Chemical Society*, 142(1):3–15, 2019.

[3] Lutz Waldecker, Roman Bertoni, Ralph Ernstorfer, and Jan Vorberger. Electron-phonon coupling and energy flow in a simple metal beyond the two-temperature approximation. *Physical Review X*, 6(2):021003, 2016.

[4] Fabio Caruso and Dino Novko. Ultrafast dynamics of electrons and phonons: from the two-temperature model to the time-dependent boltzmann equation. *arXiv preprint arXiv:2202.07237*, 2022.

[5] Pablo Maldonado, Karel Carva, Martina Flammer, and Peter M Oppeneer. Theory of out-of-equilibrium ultrafast relaxation dynamics in metals. *Physical Review B*, 96(17):174439, 2017.

[6] Shota Ono. Thermalization in simple metals: Role of electron-phonon and phonon-phonon scattering. *Physical Review B*, 97(5):054310, 2018.

[7] Hao Wang and Mo Li. Ab initio calculations of second-, third-, and fourth-order elastic constants for single crystals. *Phys. Rev. B*, 79:224102, Jun 2009.

[8] Tianqi Li. Ultrafast laser spectroscopy in complex solid state materials. *https://www.osti.gov/biblio/1226570*, 2014.

[9] Andrew M. Weiner. Ultrafast optics. *A John Wiley Sons Inc. Publication*, 2009.

[10] Zexi Lu and Xiulin Ruan. Non-equilibrium thermal transport: a review of applications and simulation approaches. *ES Energy & Environment*, 4(2):5–14, 2019.

[11] BY Mueller and B Rethfeld. Relaxation dynamics in laser-excited metals under nonequilibrium conditions. *Physical Review B*, 87(3):035139, 2013.

[12] Jia Zhang, Rui Qin, Wenjun Zhu, and Jan Vorberger. Energy relaxation and electron–phonon coupling in laser-excited metals. *Materials*, 15(5):1902, 2022.

[13] Ana M Brown, Ravishankar Sundararaman, Prineha Narang, William A Goddard III, and Harry A Atwater. Ab initio phonon coupling and optical response of hot electrons in plasmonic metals. *Physical Review B*, 94(7):075120, 2016.

[14] MI Kaganov, EM Lifshitz, and LV Tanatarov. Relaxation between electrons and the crystalline lattice. *Soviet Physics-JETP*, 4:173–178, 1957.

[15] SI Anisimov, BL Kapeliovich, TL Perelman, et al. Electron emission from metal surfaces exposed to ultrashort laser pulses. *Zh. Eksp. Teor. Fiz*, 66(2):375–377, 1974.

[16] Philip B Allen. Theory of thermal relaxation of electrons in metals. *Physical review letters*, 59(13):1460, 1987.

[17] Shota Ono. Modeling the nonthermal relaxation processes of photoexcited solids: A short review. *Transactions of the Materials Research Society of Japan*, 44(2):51–56, 2019.

[18] Viktor V Kabanov and AS Alexandrov. Electron relaxation in metals: Theory and exact analytical solutions. *Physical Review B*, 78(17):174514, 2008.

[19] Ulrike Ritzmann, Peter M Oppeneer, and Pablo Maldonado. Theory of out-of-equilibrium electron and phonon dynamics in metals after femtosecond laser excitation. *Physical Review B*, 102(21):214305, 2020.

[20] Yukiaki Ishida, Hidetoshi Masuda, Hideaki Sakai, Shintaro Ishiwata, and Shik Shin. Revealing the ultrafast light-to-matter energy conversion before heat diffusion in a layered dirac semimetal. *Physical Review B*, 93(10):100302, 2016.

[21] Shota Ono. Nonequilibrium phonon dynamics beyond the quasiequilibrium approach. *Physical Review B*, 96(2):024301, 2017.

[22] Wuli Miao and Moran Wang. Nonequilibrium effects on the electron-phonon coupling constant in metals. *Physical Review B*, 103(12):125412, 2021.

[23] WS Fann, R Storz, HWK Tom, and J Bokor. Direct measurement of nonequilibrium electron-energy distributions in subpicosecond laser-heated gold films. *Physical review letters*, 68(18):2834, 1992.

[24] B Rethfeld, A Kaiser, M Vicanek, and G Simon. Ultrafast dynamics of nonequilibrium electrons in metals under femtosecond laser irradiation. *Physical Review B*, 65(21):214303, 2002.

[25] Isabel Klett and Baerbel Rethfeld. Relaxation of a nonequilibrium phonon distribution induced by femtosecond laser irradiation. *Physical Review B*, 98(14):144306, 2018.

[26] VV Baranov and VV Kabanov. Theory of electronic relaxation in a metal excited by an ultrashort optical pump. *Physical Review B*, 89(12):125102, 2014.

[27] F Murphy-Armando, ÉD Murray, I Savić, M Trigo, D Reis, and S Fahy. Evolution of non-thermal phonon and electron populations in photo-excited germanium on picosecond timescales. *arXiv preprint arXiv:1911.12145*, 2019.

[28] Harald Ibach and Hans Lüth. *Solid-state physics: an introduction to principles of materials science*. Springer Science & Business Media, 2009.

[29] Jenő Sólyom. *Transport Phenomena*. Springer Berlin Heidelberg, Berlin, Heidelberg, 2009.

[30] J. M. Ziman. *Electrons and Phonons: The Theory of Transport Phenomena in solids*. Oxford University Press.

[31] https://web.maths.unsw.edu.au/ rsw/sphere/effsphdes/sf.html.